03-10 March 2010

TECH BRIEFS

NATIONAL AERONAUTICS AND SPACE ADMINISTRATION

INTRODUCTION

Tech Briefs are short announcements of innovations originating from research and development activities of the National Aeronautics and Space Administration. They emphasize information considered likely to be transferable across industrial, regional, or disciplinary lines and are issued to encourage commercial application.

Availability of NASA Tech Briefs and TSPs

Requests for individual Tech Briefs or for Technical Support Packages (TSPs) announced herein should be addressed to

National Technology Transfer Center

Telephone No. **(800) 678-6882** or via World Wide Web at **www.nttc.edu**

Please reference the control numbers appearing at the end of each Tech Brief. Information on NASA's Innovative Partnerships Program (IPP), its documents, and services is also available at the same facility or on the World Wide Web at **http://www.nasa.gov/offices/ipp/network/index.html**

Innovative Partnerships Offices are located at NASA field centers to provide technology-transfer access to industrial users. Inquiries can be made by contacting NASA field centers listed below.

NASA Field Centers and Program Offices

Ames Research Center
Lisa L. Lockyer
(650) 604-1754
lisa.l.lockyer@nasa.gov

Dryden Flight Research Center
Gregory Poteat
(661) 276-3872
greg.poteat@dfrc.nasa.gov

Glenn Research Center
Kathy Needham
(216) 433-2802
kathleen.k.needham@nasa.gov

Goddard Space Flight Center
Nona Cheeks
(301) 286-5810
nona.k.cheeks@nasa.gov

Jet Propulsion Laboratory
Andrew Gray
(818) 354-3821
gray@jpl.nasa.gov

Johnson Space Center
information
(281) 483-3809
jsc.techtran@mail.nasa.gov

Kennedy Space Center
David R. Makufka
(321) 867-6227
david.r.makufka@nasa.gov

Langley Research Center
Brian Beaton
(757) 864-2192
brian.f.beaton@nasa.gov

Marshall Space Flight Center
Jim Dowdy
(256) 544-7604
jim.dowdy@msfc.nasa.gov

Stennis Space Center
Ramona Travis
(228) 688-3832
ramona.e.travis@nasa.gov

Carl Ray, Program Executive
Small Business Innovation Research (SBIR) & Small Business Technology Transfer (STTR) Programs
(202) 358-4652
carl.g.ray@nasa.gov

Doug Comstock, Director
Innovative Partnerships Program Office
(202) 358-2560
doug.comstock@nasa.gov

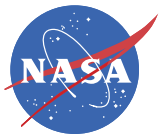

TECH BRIEFS

NATIONAL AERONAUTICS AND SPACE ADMINISTRATION

Software Tool Integrating Data Flow Diagrams and Petri Nets

Lyndon B. Johnson Space Center, Houston, Texas

Data Flow Diagram – Petri Net (DFPN) is a software tool for analyzing other software to be developed. The full name of this program reflects its design, which combines the benefit of data-flow diagrams (which are typically favored by software analysts) with the power and precision of Petri-net models, without requiring specialized Petri-net training. (A Petri net is a particular type of directed graph, a description of which would exceed the scope of this article.)

DFPN assists a software analyst in drawing and specifying a data-flow diagram, then translates the diagram into a Petri net, then enables graphical tracing of execution paths through the Petri net for verification, by the end user, of the properties of the software to be developed. In comparison with prior means of verifying the properties of software to be developed, DFPN makes verification by the end user more nearly certain, thereby making it easier to identify and correct misconceptions earlier in the development process, when correction is less expensive. After the verification by the end user, DFPN generates a printable system specification in the form of descriptions of processes and data.

This work was done by Carroll Thronesbery of S&K Technologies and Madjid Tavana of LaSalle University for Johnson Space Center. Further information is contained in a TSP (see page 1). MSC-23242

Adaptive Nulling for Interferometric Detection of Planets

Deep nulls would be obtained despite optical imperfections.

NASA's Jet Propulsion Laboratory, Pasadena, California

An adaptive-nulling method has been proposed to augment the nulling-optical-interferometry method of detection of Earth-like planets around distant stars. The method is intended to reduce the cost of building and aligning the highly precise optical components and assemblies needed for nulling.

Typically, at the mid-infrared wavelengths used for detecting planets orbiting distant stars, a star is millions of times brighter than an Earth-sized planet. In order to directly detect the light from the planet, it is necessary to remove most of the light coming from the star. Nulling interferometry is one way to suppress the light from the star without appreciably suppressing the light from the planet.

In nulling interferometry in its simplest form, one uses two nominally identical telescopes aimed in the same direction and separated laterally by a suitable distance. The light collected by the two telescopes is processed through optical trains and combined on a detector. The optical trains are designed such that the electric fields produced by an on-axis source (the star) are in anti-phase at the detector while the electric fields from the planet, which is slightly off-axis, combine in phase, so that the contrast ratio between the star and the planet is greatly decreased. If the electric fields from the star are exactly equal in amplitude and opposite in phase, then the star is effectively "nulled out."

Nulling is effective only if it is complete in the sense that it occurs simultaneously in both polarization states and at all wavelengths of interest. The need to ensure complete nulling translates to extremely tight demands upon the design and fabrication of the complex optical trains: The two telescopes must be highly symmetric, the reflectivities of the many mirrors in the telescopes and other optics must be carefully tailored, the optical coatings must be extremely uniform, sources of contamination must be minimized, optical surfaces must be nearly ideal, and alignments must be extremely precise. Satisfaction of all of these requirements entails substantial cost.

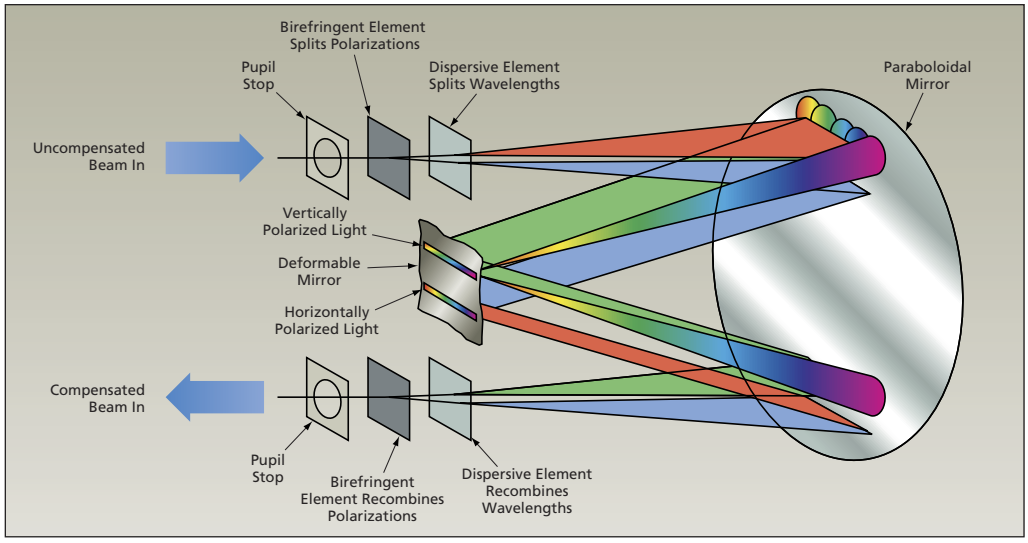

Light Would Be Decomposed into wavelength and polarization components, the phases and amplitudes of which would be controlled by use of a deformable mirror. The components would then be recombined to obtain a compensated beam.

In the proposed method, a compensator would be inserted into each optical train, upstream of the location where the output beam from the two telescopes are combined. Each compensator would be an optical subsystem that would control the amplitude and phase of the electric field of the spatial mode that couples into the detector, and would do so independently at each wavelength for each of the two polarization states of the beam. The compensator would correct for the imperfections in the optical train and in the beam combiner, making it possible to obtain a deep null from an imperfect instrument.

In one conceptual compensator (see figure), the uncompensated beam from the telescope would be split by a birefringent optical element into vertically and horizontally polarized components, which would be dispersed into wavelength components. The light of the various wavelength components would be focused by a paraboloidal mirror onto a deformable mirror, forming two bright lines, each corresponding to the dispersed spectrum for each polarization state. That is to say, each combination of polarization and wavelength would be focused to a different point on the mirror. The local piston displacement and local slope of the deformable mirror would be controlled to control the phase and amplitude, respectively. Then the light would be re-collimated by the paraboloidal mirror, the wavelength components would be recombined by another dispersive optical element, and then the horizontal and vertical polarization components would be recombined by another birefringent element to produce a single, corrected output beam. The sensing of the amplitude and phase errors and the control of the deformable mirror would be effected by use of a combination of previously developed nulling and wavefront-sensing-and-control techniques. This approach has been successfully demonstrated in the laboratory, both at near-infrared and mid-infrared wavelengths.

This work was done by Oliver P. Lay and Robert D. Peters of Caltech for NASA's Jet Propulsion Laboratory. Further information is contained in a TSP (see page 1). NPO-40152

Reducing the Volume of NASA Earth-Science Data

NASA's Jet Propulsion Laboratory, Pasadena, California

A computer program reduces data generated by NASA Earth-science missions into representative clusters characterized by centroids and membership information, thereby reducing the large volume of data to a level more amenable to analysis. The program effects an autonomous data-reduction/clustering process to produce a representative distribution and joint relationships of the data, without assuming a specific type of distribution and relationship and without resorting to domain-specific knowledge about the data.

The program implements a combination of a data-reduction algorithm known as the entropy-constrained vector quantization (ECVQ) and an optimization algorithm known as the differential evolution (DE). The combination of algorithms generates the Pareto front of clustering solutions that presents the compromise between the quality of the reduced data and the degree of reduction.

Similar prior data-reduction computer programs utilize only a clustering algorithm, the parameters of which are tuned manually by users. In the present program, autonomous optimization of the parameters by means of the DE supplants the manual tuning of the parameters. Thus, the program determines the best set of clustering solutions without human intervention.

This program was written by Seungwon Lee, Amy J. Braverman, and Alexandre Guillaume of Caltech for NASA's Jet Propulsion Laboratory. Further information is contained in a TSP (see page 1).

This software is available for commercial licensing. Please contact Karina Edmonds of the California Institute of Technology at (626) 395-2322. Refer to NPO-45583.

Reception of Multiple Telemetry Signals via One Dish Antenna

Telemetry signals coming from slightly different directions can be separated.

NASA's Jet Propulsion Laboratory, Pasadena, California

A microwave aeronautical-telemetry receiver system includes an antenna comprising a seven-element planar array of receiving feed horns centered at the focal point of a paraboloidal dish reflector that is nominally aimed at a single aircraft or at multiple aircraft flying in formation. Through digital processing of the signals received by the seven feed horns, the system implements a method of enhanced cancellation of interference, such that it becomes possible to receive telemetry signals in the same frequency channel simultaneously from either or both of two aircraft at slightly different angular positions within the field of view of the antenna, even in the presence of multipath propagation.

The present system is an advanced version of the system described in "Spatio-Temporal Equalizer for a Receiving-Antenna Feed Array" NPO-43077, *NASA Tech Briefs*, Vol. 34, No. 2 (February 2010), page 32. To recapitulate: The radio-frequency telemetry signals received by the seven elements of the array are digitized, converted to complex baseband form, and sent to a spatio-temporal equalizer that consists mostly of a bank of seven adaptive finite-impulse-response (FIR) filters (one for each element in the array) plus a unit that sums the outputs of the filters. The combination of the spatial diversity of the feed-horn array and the temporal diversity of the filter bank affords better multipath-suppression performance than is achievable by means of temporal equalization alone. The FIR filter bank adapts itself in real time to enable reception of telemetry at a low bit error rate, even in the

presence of frequency-selective multipath propagation like that commonly found at flight-test ranges.

The combination of the array and the filter bank makes it possible to constructively add multipath incoming signals to the corresponding directly arriving signals, thereby enabling reductions in telemetry bit-error rates. The combination of the array and the filter bank also makes it possible to extract, in real time, pointing information that can be used to identify both the main beam(s) traveling directly from the target aircraft and the beam(s) that reach the antenna after reflection from the ground. Information on the relative amplitudes and phases of the incoming signals, which is indicative of the difference between the antenna pointing direction and the actual directions of the direct and reflected beams, is contained in the adaptive FIR weights. This information is fed to an angle estimator, which generates instantaneous estimates of the difference between the antenna-pointing and target directions. The time series of these estimates is sent to a set of Kalman filters, which perform smoothing and prediction of the time series and extract velocity and acceleration estimates from the time series. The outputs of the Kalman filters are sent to a unit that controls the pointing of the antenna.

For the purposes of the present system, each telemetry signal is assumed to be conveyed by a constant-envelope phase modulation, known among specialists as SOQPSK-TG, that is commonly used on flight-test telemetry ranges. The main distinction between the present and previously reported versions of this system lies in the algorithm governing the adaptation of the FIR filters. In the previously reported version of this system, the filter weights would be adapted by an algorithm, known in the art as the constant-modulus algorithm (CMA), which tends to lock onto the strongest constant-envelope signal while suppressing others.

The algorithm used in present system, denoted the interference-canceling constant-modulus algorithm (IC-MA), is an extended version of the CMA. The IC-CMA goes beyond the CMA by incorporating adaptive interference-canceling and multiple-beam-forming subalgorithms. Unlike the CMA, the IC-CMA does not lock onto a single signal: instead, utilizing adaptive estimates of cross-correlations between signals, it separates two interfering telemetry signals, making it possible to utilize both of them or, if desired, to ignore one of them. In addition, if multiple signals are present and the stronger ones are deliberately suppressed in early stages of IC-CMA processing, then weaker signals can sometimes be recovered.

This work was done by Ryan Mukai and Victor Vilnrotter of Caltech for NASA's Jet Propulsion Laboratory. Further information is contained in a TSP (see page 1).

In accordance with Public Law 96-517, the contractor has elected to retain title to this invention. Inquiries concerning rights for its commercial use should be addressed to:

Innovative Technology Assets Management
JPL
Mail Stop 202-233
4800 Oak Grove Drive
Pasadena, CA 91109-8099
E-mail: iaoffice@jpl.nasa.gov

Refer to NPO-44079, volume and number of this NASA Tech Briefs *issue, and the page number.*

Space-Qualified Traveling-Wave Tube

TWT was developed for use as a high-power microwave amplifier for high-rate transmission of data.

John H. Glenn Research Center, Cleveland, Ohio

The L-3 Communications Electron Technologies, Inc. Model 999HA traveling-wave tube (TWT), was developed for use as a high-power microwave amplifier for high-rate transmission of data and video signals from deep space to Earth (see figure). The 999HA is a successor to the 999H — a non-space-qualified TWT described in "High-Power, High-Efficiency Ka-Band Traveling-Wave Tube" (LEW-17900-1), *NASA Tech Briefs*, Vol. 31, No. 2 (February 2007), page 32. Operating in the 31.8-to-32.3 GHz frequency band, the 999HA has been shown to generate 252 W of continuous-wave output power at 62 percent overall power efficiency — a 75-percent increase in output power over the 999H.

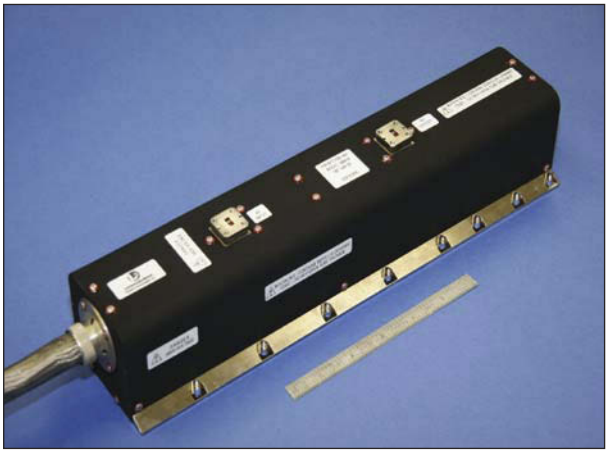

A **Photo of the TWT** shows its approximate dimensions. [The ruler below is 6 in. (≈15 cm) long.]

The mass of the 999HA is 35 percent less than that of the 999H. Moreover, taking account of the elimination of a Faraday cage that is necessary for operation of the 999H but is obviated by a redesign of high-voltage feedthroughs for the 999HA, the overall reduction in mass becomes 57 percent with an 82 percent reduction in volume. Through a series of rigorous tests, the 999HA has been qualified for operation aboard spacecraft with a lifetime exceeding seven years. Offspring of the 999HA will fly on the Kepler and Lunar Reconnaissance Orbiter missions.

This work was done by Jeffrey D. Wilson, Richard Krawczyk, Rainee N. Simons, and Wallace D. Williams of Glenn Research Center and Neal R. Robbins, Daniel R. Dibb, William L. Menninger, Xiaoling Zhai, and Robert T. Benton of L-3 Communications Electron Technologies, Inc. Further information is contained in a TSP (see page 1).

Inquiries concerning rights for the commercial use of this invention should be addressed to NASA Glenn Research Center, Innovative Partnerships Office, Attn: Steve Fedor, Mail Stop 4–8, 21000 Brookpark Road, Cleveland, Ohio 44135. Refer to LEW-18220-1.

Smart Power Supply for Battery-Powered Systems

This power supply can be used in remote vehicles, or for any application requiring battery power or battery charging.

John H. Glenn Research Center, Cleveland, Ohio

A power supply for battery-powered systems has been designed with an embedded controller that is capable of monitoring and maintaining batteries, charging hardware, while maintaining output power. The power supply is primarily designed for rovers and other remote science and engineering vehicles, but it can be used in any battery alone, or battery and charging source applications. The supply can function autonomously, or can be connected to a host processor through a serial communications link. It can be programmed *a priori* or on the fly to return current and voltage readings to a host.

It has two output power busses: a constant 24-V direct current nominal bus, and a programmable bus for output from approximately 24 up to approximately 50 V. The programmable bus voltage level, and its output power limit, can be changed on the fly as well. The power supply also offers options to reduce the programmable bus to 24 V when the set power limit is reached, limiting output power in the case of a system fault detected in the system.

The smart power supply is based on an embedded 8051-type single-chip microcontroller. This choice was made in that a credible progression to flight (radiation hard, high reliability) can be assumed as many 8051 processors or gate arrays capable of accepting 8051-type core presently exist and will continue to do so for some time.

To solve the problem of centralized control, this innovation moves an embedded microcontroller to the power supply and assigns it the task of overseeing the operation and charging of the power supply assets. This embedded processor is connected to the application central processor via a serial data link such that the central processor can request updates of various parameters within the supply, such as battery current, bus voltage, remaining power in battery estimations, etc. This supply has a direct connection to the battery bus for common (quiescent) power application. Because components from multiple vendors may have

differing power needs, this supply also has a secondary power bus, which can be programmed *a priori* or on-the-fly to boost the primary battery voltage level from 24 to 50 V to accommodate various loads as they are brought on line. Through voltage and current monitoring, the device can also shield the charging source from overloads, keep it within safe operating modes, and can meter available power to the application and maintain safe operations.

This work was done by Michael J. Krasowski, Lawrence C. Greer, and Norman F. Prokop of Glenn Research Center and Joseph M. Flatico of Ohio Aerospace Institute. Further information is contained in a TSP (see page 1).

Inquiries concerning rights for the commercial use of this invention should be addressed to NASA Glenn Research Center, Innovative Partnerships Office, Attn: Steve Fedor, Mail Stop 4–8, 21000 Brookpark Road, Cleveland, Ohio 44135. Refer to LEW-18317-1.

Parallel Processing of Broad-Band PPM Signals

Timing-error correction is independent of timing-error estimation.

NASA's Jet Propulsion Laboratory, Pasadena, California

A parallel-processing algorithm and a hardware architecture to implement the algorithm have been devised for time-slot synchronization in the reception of pulse-position-modulated (PPM) optical or radio signals. As in the cases of some prior algorithms and architectures for parallel, discrete-time, digital processing of signals other than PPM, an incoming broadband signal is divided into multiple parallel narrower-band signals by means of sub-sampling and filtering. The number of parallel streams is chosen so that the frequency content of the narrower-band signals is low enough to enable processing by relatively-low-speed complementary metal oxide semiconductor (CMOS) electronic circuitry.

The algorithm and architecture are intended to satisfy requirements for time-varying time-slot synchronization and post-detection filtering, with correction of timing errors independent of estimation of timing errors. They are also intended to afford flexibility for dynamic reconfiguration and upgrading. The architecture is implemented in a reconfigurable CMOS processor in the form of a field-programmable gate array. The algorithm and its hardware implementation incorporate three separate time-varying filter banks for three distinct functions: correction of sub-sample timing errors, post-detection filtering, and post-detection estimation of timing errors. The design of the filter bank for correction of timing errors, the method of estimating timing errors, and the design of a feedback-loop filter are governed by a host of parameters, the most critical one, with regard to processing very broadband signals with CMOS hardware, being the number of parallel streams (equivalently, the rate-reduction parameter).

This work was done by Andrew Gray, Edward Kang, Norman Lay, Victor Vilnrotter, Meera Srinivasan, and Clement Lee of Caltech for NASA's Jet Propulsion Laboratory.

In accordance with Public Law 96-517, the contractor has elected to retain title to this invention. Inquiries concerning rights for its commercial use should be addressed to:

Innovative Technology Assets Management
JPL
Mail Stop 202-233
4800 Oak Grove Drive
Pasadena, CA 91109-8099
E-mail: iaoffice@jpl.nasa.gov

Refer to NPO-40711, volume and number of this NASA Tech Briefs *issue, and the page number.*

Inexpensive Implementation of Many Strain Gauges

Arrays of metal film resistors would sense strains at multiple locations.

NASA's Jet Propulsion Laboratory, Pasadena, California

It has been proposed to develop arrays of strain gauges as arrays of ordinary metal film resistors and associated electronic readout circuitry on printed-circuit boards or other suitable substrates. This proposal is a by-product of a development of instrumentation utilizing metal film resistors on printed-circuit boards to measure temperatures at multiple locations. In the course of that development, it was observed that in addition to being sensitive to temperature, the metal film resistors were also sensitive to strains in the printed-circuit boards to which they were attached. Because of the low cost of ordinary metal film resistors (typically <$0.01 apiece at 2007 prices), the proposal could enable inexpensive implementation of arrays of many (e.g., 100 or more) strain gauges, possibly concentrated in small areas. For example, such an array could be designed for use as a computer keyboard with no moving parts, as a device for sensing the shape of an object resting on a surface, or as a device for measuring strains at many points on a mirror, a fuel tank, an airplane wing, or other large object.

Ordinarily, the effect of strain on resistance would be regarded as a nuisance in a temperature-measuring application, and the effect of temperature on resistance would be regarded as a nuisance in a strain-measuring application. The strain-induced changes in resistance of the metal film resistors in question are less than those of films in traditional strain gauges. The main novel aspect of present proposal lies in the use of circuitry affording sufficient sensitivity to measure strain plus means for compensating for the effect of temperature.

For an array of metal film resistors used as proposed, the readout circuits would include a high-accuracy analog-to-digital converter fed by a low noise current source, amplifier chain, and an analog multiplexer chain. Corrections would be provided by use of

high-accuracy calibration resistors and a temperature sensor. By use of such readout circuitry, it would be possible to read the resistances of as many as 100 fixed resistors in a time interval of 1 second at a resolution much greater than 16 bits. The readout data would be processed, along with temperature calibration data, to deduce the strain on the printed-circuit board or other substrate in the areas around the resistors. It should also be possible to also deduce the temperature from the readings.

This work was done by Andrew C. Berkun of Caltech for NASA's Jet Propulsion Laboratory. For more information, contact iaoffice@jpl.nasa.gov. NPO-45711

Constant-Differential-Pressure Two-Fluid Accumulator

An improved design does not rely on the spring rate of the accumulator tank.

John H. Glenn Research Center, Cleveland, Ohio

A two-fluid accumulator has been designed, built, and demonstrated to provide an acceptably close approximation to constant differential static pressure between two fluids over the full ranges of (1) accumulator stroke, (2) rates of flow of the fluids, and (3) common static pressure applied to the fluids. Prior differential-pressure two-fluid accumulators are generally not capable of maintaining acceptably close approximations to constant differential pressures.

The inadequacies of a typical prior differential-pressure two-fluid accumulator can be summarized as follows: The static differential pressure is governed by the intrinsic spring rate (essentially, the stiffness) of an accumulator tank. The spring rate can be tailored through selection of the tank-wall thickness, selection of the number and/or shape of accumulator convolutions, and/or selection of accumulator material(s). Reliance on the intrinsic spring rate of the tank results in three severe limitations:

(1) The spring rate and the expulsion efficiency tend to be inversely proportional to each other: that is to say, as the stiffness (and thus the differential pressure) is increased, the range of motion of the accumulator is reduced.

(2) As the applied common static pressure increases, the differential pressure tends to decrease. An additional disadvantage, which may or may not be considered limiting, depending on the specific application, is that an increase in stiffness entails an increase in weight.

(3) The additional weight required by a low expulsion efficiency accumulator eliminates the advantage given to such gas storage systems. The high expulsion efficiency provided by this two-fluid accumulator allows for a lightweight, tightly packaged system, which can be used in conjunction with a fuel-cell-based system.

The design of the present two-fluid accumulator does not rely on the intrinsic spring rate of an accumulator tank to establish the differential pressure. Instead, the accumulator tank is a relatively rigid cylinder, within which is placed a bellows that separates the two fluids. A constant-force spring pulls on the end plate of the bellows, as though the end plate were a piston. This spring action, applied over the area of the end plate, results in the desired differential pressure. The differential pressure can closely approximate a constant value because the constant spring force is at least an order of magnitude greater than the spring rate of the bellows. As a result, for challenging differential pressures below 5 psi (34.5 kPa), this new design can achieve a stroke that permits greater than 75 percent expulsion efficiency with an absolute operating pressure as high as 2,400 psig (≈16.6 MPa) and maintain the differential pressure within 10 percent of the nominal. The separate spring assembly also permits the differential pressure to be customized with whatever constant-force springs can be manufactured. The outer cylindrical housing can be made of a number of lightweight materials as the application requires. An example of prior art had 50 percent variability in differential pressure over a short stroke that permitted less than 10 percent expulsion efficiency with an absolute operating pressure of only 150 psig (≈1.14 MPa).

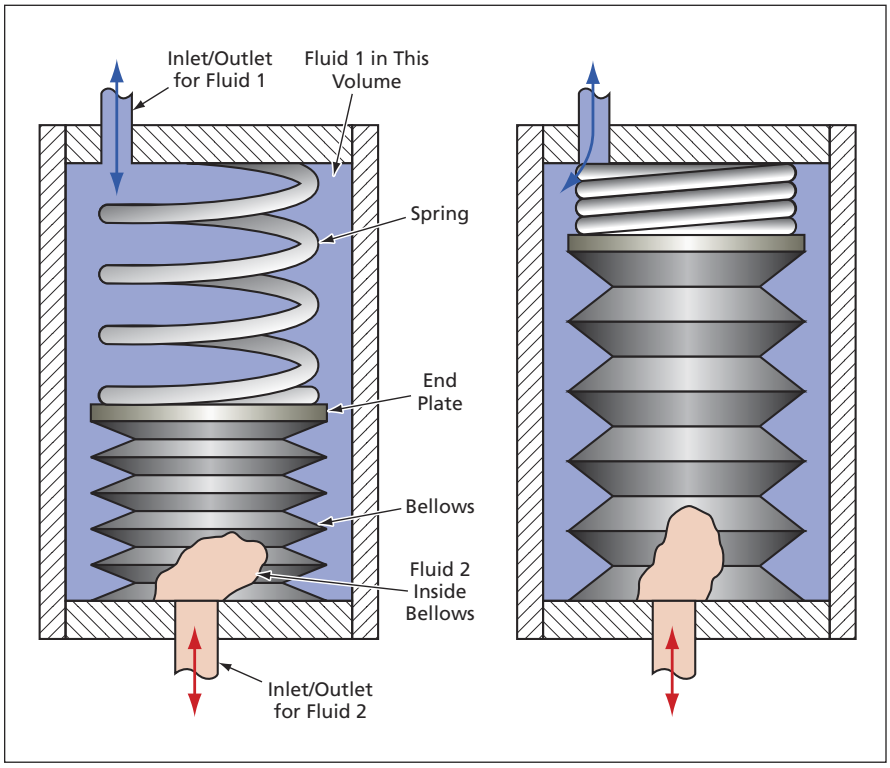

The **Spring Exerts an Approximately Constant Force** on the bellows throughout the stroke range, thereby maintaining approximately constant differential pressure between fluids 1 and 2.

This work was done by Benjamin Piecuch and Luke T. Dalton of Proton Energy Systems, Inc. for Glenn Research Center.

Inquiries concerning rights for the commercial use of this invention should be addressed to NASA Glenn Research Center, Innovative Partnerships Office, Attn: Steve Fedor, Mail Stop 4–8, 21000 Brookpark Road, Cleveland, Ohio 44135. Refer to LEW-18133-1.

Inflatable Tubular Structures Rigidized With Foams

Lightweight booms could be deployed from compact stowage and rigidized in place.

Marshall Space Flight Center, Alabama

Inflatable tubular structures that have annular cross sections rigidized with foams, and the means of erecting such structures in the field, are undergoing development. Although the development effort has focused on lightweight structural booms to be transported in compact form and deployed in outer space, the principles of design and fabrication are also potentially applicable to terrestrial structures, including components of ultralightweight aircraft, lightweight storage buildings and shelters, lightweight insulation, and sales displays.

The use of foams to deploy and harden inflatable structures was first proposed as early as the 1960s, and has been investigated in recent years by NASA, the U.S. Air Force Research Laboratory, industry, and academia. In cases of deployable booms, most of the investigation in recent years has focused on solid cross sections, because they can be constructed relatively easily. However, solid-section foam-filled booms can be much too heavy for some applications.

In contrast, booms with annular cross sections according to the present innovation can be tailored to obtain desired combinations of stiffness and weight through choice of diameters, wall thicknesses, and foam densities. By far the most compelling advantage afforded by this innovation is the possibility of drastically reducing weights while retaining or increasing the stiffnesses, relative to comparable booms that have solid foam-filled cross sections.

A typical boom according to this innovation includes inner and outer polyimide film sleeves to contain foam that is injected between them during deployment. The cavity inside the inner polyimide sleeve is pressurized for deployment (see figure). The internal pressure provides out-of-plane stiffness for the inner sleeve, preventing its collapse and thereby creating the barrier needed to maintain the radially innermost surface of the injected foam in the desired cylindrical shape during expansion and curing of the foam.

Lightweight end plugs seal the ends of the boom. The plugs contain inlets for compressed air and the foam; they also contain escape ports for gas generated during expansion of the foam. Lightweight flexible hoses are used to inflate the interior of the boom and to inject the foam.

In preparation for a typical application, an assembly of sleeves and end plugs destined to be deployed and rigidized into a boom would be packaged compactly, the inner and outer sleeves being accordion-folded into a storage canister. For deployment, compressed air would be admitted to the cavity enclosed by the inner sleeve. While this cavity remained pressurized, the foam would be injected into the space between the inner and outer sleeves. Once the injected foam had cured, the internal pressure would be released and the boom would be ready for service.

This work was done by Michael L. Tinker of Marshall Space Flight Center and Andrew R. Schnell of Tennessee Technological University. For further information, contact Sammy Nabors, MSFC Commercialization Assistance Lead, at sammy.a.nabors@nasa.gov. Refer to MFS-31776-1.

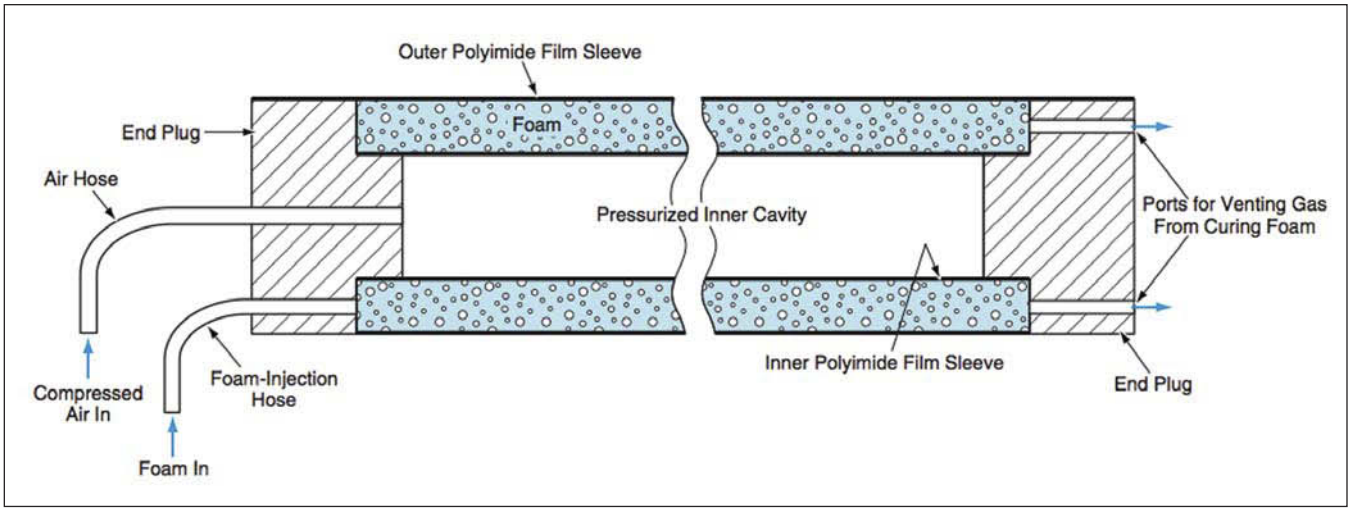

Foam Is Injected into the annular space between the inner and outer polyimide film sleeves while the inner cavity remains pressurized. After curing of the injected foam to a state of rigidity, the pressure is released, and the boom holds its shape.

Power Generator With Thermo-Differential Modules

Lyndon B. Johnson Space Center, Houston, Texas

A thermoelectric power generator consists of an oven box and a solar cooker/solar reflector unit. The solar reflector concentrates sunlight into heat and transfers the heat into the oven box via a heat pipe. The oven box unit is surrounded by five thermoelectric modules and is located at the bottom end of the solar reflector. When the heat is pumped into one side of the thermoelectric module and ejected from the opposite side at ambient temperatures, an electrical current is produced.

Typical temperature accumulation in the solar reflector is approximately 200 °C (392 °F). The heat pipe then transfers heat into the oven box with a loss of about 40 percent. At the ambient temperature of about 20 °C (68 °F), the temperature differential is about 100 °C (180 °F) apart. Each thermoelectric module, generates about 6 watts of power. One oven box with five thermoelectric modules produces about 30 watts.

The system provides power for unattended instruments in remote areas, such as space colonies and space vehicles, and in polar and other remote regions on Earth.

This work was done by John R. Saiz of Johnson Space Center and James Nguyen of Jacobs-Sverdrup. Further information is contained in a TSP (see page 1).
MSC-24268-1

Mechanical Extraction of Power From Ocean Currents and Tides

No electrical equipment would be submerged in the ocean.

NASA's Jet Propulsion Laboratory, Pasadena, California

A proposed scheme for generating electric power from rivers and from ocean currents, tides, and waves is intended to offer economic and environmental advantages over prior such schemes, some of which are at various stages of implementation, others of which have not yet advanced beyond the concept stage. This scheme would be less environmentally objectionable than are prior schemes that involve the use of dams to block rivers and tidal flows. This scheme would also not entail the high maintenance costs of other proposed schemes that call for submerged electric generators and cables, which would be subject to degradation by marine growth and corrosion.

A basic power-generation system according to the scheme now proposed would not include any submerged electrical equipment. The submerged portion of the system would include an all-mechanical turbine/pump unit that would superficially resemble a large land-based wind turbine (see figure). The turbine axis would turn slowly as it captured energy from the local river flow, ocean current, tidal flow, or flow from an ocean-wave device. The turbine axis would drive a pump through a gearbox to generate an enclosed flow of water, hydraulic fluid, or other suitable fluid at a relatively high pressure [typically ≈500 psi (≈3.4 MPa)].

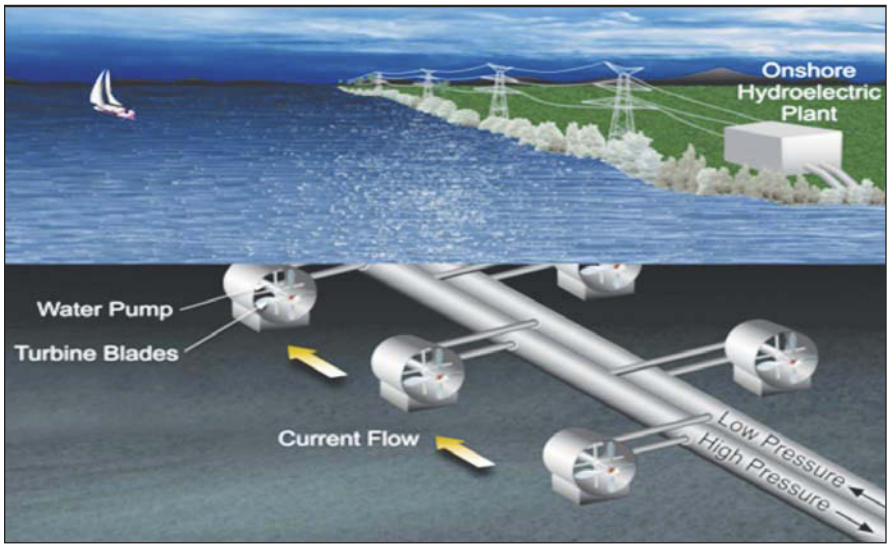

Turbine Blades Would Intercept Flow in the ocean or other natural body of water. The turbine would drive a pump to obtain a smaller, higher-pressure flow that would be piped to an above-water facility for use in generating electric power.

The pressurized fluid could be piped to an onshore or offshore facility, above the ocean surface, where it would be used to drive a turbine that, in turn, would drive an electric generator. The fluid could be recirculated between the submerged unit and the power-generation facility in a closed flow system; alternatively, if the fluid were seawater, it could be taken in from the ocean at the submerged turbine/pump unit and discharged back into the ocean from the power-generation facility. Another alternative would be to use the pressurized flow to charge an elevated reservoir or other pumped-storage facility, from whence fluid could later be released to

drive a turbine/generator unit at a time of high power demand.

Multiple submerged turbine/pump units could be positioned across a channel to extract more power than could be extracted by a single unit. In that case, the pressurized flows in their output pipes would be combined, via check valves, into a wider pipe that would deliver the combined flow to a power-generating or pumped-storage facility.

This work was done by Jack Jones and Yi Chao of Caltech for NASA's Jet Propulsion Laboratory. Further information is contained in a TSP (see page 1). ***v***

In accordance with Public Law 96-517, the contractor has elected to retain title to this invention. Inquiries concerning rights for its commercial use should be addressed to:

Innovative Technology Assets Management
JPL
Mail Stop 202-233
4800 Oak Grove Drive
Pasadena, CA 91109-8099
E-mail: iaoffice@jpl.nasa.gov

Refer to NPO-45174, volume and number of this NASA Tech Briefs *issue, and the page number.*

Nitrous Oxide/Paraffin Hybrid Rocket Engines

Thrusts can exceed those of engines that burn HTPB fuels.

Marshall Space Flight Center, Alabama

Nitrous oxide/paraffin (N_2OP) hybrid rocket engines have been invented as alternatives to other rocket engines — especially those that burn granular, rubbery solid fuels consisting largely of hydroxyl-terminated polybutadiene (HTPB). Originally intended for use in launching spacecraft, these engines would also be suitable for terrestrial use in rocket-assisted takeoff of small airplanes. The main novel features of these engines are (1) the use of reinforced paraffin as the fuel and (2) the use of nitrous oxide as the oxidizer.

Hybrid (solid-fuel/fluid-oxidizer) rocket engines offer advantages of safety and simplicity over fluid-bipropellant (fluid-fuel/fluid-oxidizer) rocket engines, but the thrusts of HTPB-based hybrid rocket engines are limited by the low regression rates of the fuel grains. Paraffin used as a solid fuel has a regression rate about 4 times that of HTPB, but pure paraffin fuel grains soften when heated; hence, paraffin fuel grains can, potentially, slump during firing. In a hybrid engine of the present type, the paraffin is molded into a 3-volume-percent graphite sponge or similar carbon matrix, which supports the paraffin against slumping during firing. In addition, because the carbon matrix material burns along with the paraffin, engine performance is not appreciably degraded by use of the matrix.

The use of nitrous oxide as the oxidizer offers the following advantages:

- Because nitrous oxide is non-toxic, the extra precautions for handling of toxic oxidizers are unnecessary.
- Unlike liquid oxygen, nitrous oxide can safely be stored for indefinitely long times under non-cryogenic conditions: for example, it can be stored at 0.7 the density of water at a pressure of 700 psi (≈4.8 MPa) at a temperature of 20 °C.
- Because it can be stored non-cryogenically, nitrous oxide can be stored in a rocket prior to launch, making it possible to launch in less time than would be required if it were necessary to transfer the oxidizer fluid from cryogenic storage.
- Nitrous oxide can serve as its own autogenous pressurant gas, eliminating the need for the high-pressure helium tanks that are necessary for pressurizing propellant fluids in fluid-bipropellant and hybrid rocket engines of prior design. The elimination of the helium tanks and associated plumbing increases reliability while reducing mass and cost.
- Subcooled liquid nitrous oxide could be used as a propellant in upper rocket stages to reduce upper-stage engine masses and thereby enable increases in payloads. Alternatively, subcooled nitrous oxide could be used with oxygen pressurant to increase the specific impulses achievable at given tank weights.

Another advantage is the potential to use nitrous oxide as a monopropellant, in place of hydrazine. Although the specific impulse achievable by use of nitrous oxide is somewhat lower than that achievable by use of hydrazine, cost would be reduced and safety enhanced by elimination of the toxic hazard posed by hydrazine.

Yet another alternative would be to utilize catalytic decomposition of nitrous oxide in a monopropellant reactor to effect a hybrid ignition system. The exhaust of a nitrous oxide from a monopropellant reactor is a 2:1 N_2/O_2 mixture at a temperature of 1,200 °C. This exhaust can be used to ignite a hybrid propellant as many times as desired, making it possible to restart a stopped hybrid rocket engine.

This work was done by Robert Zubrin and Gary Snyder of Pioneer Astronautics for Marshall Space Flight Center.

For further information, contact Sammy Nabors, MSFC Commercialization Assistance Lead, at sammy.a.nabors@nasa.gov. Refer to MFS-32542-1.

Optimized Li-Ion Electrolytes Containing Fluorinated Ester Co-Solvents

Resulting rechargeable batteries could be used in consumer electronics, electric cars, and scientific instrumentation in extreme environments.

NASA's Jet Propulsion Laboratory, Pasadena, California

A number of experimental lithium-ion cells, consisting of MCMB (mesocarbon microbeads) carbon anodes and $LiNi_{0.8}Co_{0.2}O_2$ cathodes, have been fabricated with increased safety and expanded capability. These cells serve to verify and demonstrate the reversibility, low-temperature performance, and electrochemical aspects of each electrode as determined from a number of electrochemical characterization techniques. A number of Li-ion electrolytes possessing fluorinated ester co-solvents, namely trifluoroethyl butyrate (TFEB) and trifluoroethyl propionate (TFEP), were demonstrated to deliver good performance over a wide temperature range in experimental lithium-ion cells.

The general approach taken in the development of these electrolyte formulations is to optimize the type and composition of the co-solvents in ternary and quaternary solutions, focusing upon adequate stability [i.e., EC (ethylene carbonate) content needed for anode passivation, and EMC (ethyl methyl carbonate) content needed for lowering the viscosity and widening the temperature range, while still providing good stability], enhancing the inherent safety characteristics (incorporation of fluorinated esters), and widening the temperature range of operation (the use of both fluorinated and non-fluorinated esters). Furthermore, the use of electrolyte additives, such as VC (vinylene carbonate) [solid electrolyte interface (SEI) promoter] and DMAc (thermal stabilizing additive), provide enhanced high-temperature life characteristics.

Multi-component electrolyte formulations enhance performance over a temperature range of –60 to +60 °C. With the need for more safety with the use of these batteries, flammability was a consideration. One of the solvents investigated, TFEB, had the best performance with improved low-temperature capability and high-temperature resilience. This work optimized the use of TFEB as a co-solvent by developing the multi-component electrolytes, which also contain non-halogenated esters, film forming additives, thermal stabilizing additives, and flame retardant additives.

Further optimization of these electrolyte formulations is anticipated to yield improved performance. It is also anticipated that much improved performance will be demonstrated once these electrolyte solutions are incorporated into hermetically sealed, large capacity prototype cells, especially if effort is devoted to ensure that all electrolyte components are highly pure.

This work was done by G. K. Surya Prakash of the University of Southern California and Marshall Smart, Kiah Smith, and Ratnakumar Bugga of Caltech for NASA's Jet Propulsion Laboratory. Further information is contained in a TSP (see page 1).

In accordance with Public Law 96-517, the contractor has elected to retain title to this invention. Inquiries concerning rights for its commercial use should be addressed to:

Innovative Technology Assets Management
JPL
Mail Stop 202-233
4800 Oak Grove Drive
Pasadena, CA 91109-8099
E-mail: iaoffice@jpl.nasa.gov

Refer to NPO-45824, volume and number of this NASA Tech Briefs *issue, and the page number.*

Probabilistic Multi-Factor Interaction Model for Complex Material Behavior

Complex material behavior is represented by a single equation of product form.

John H. Glenn Research Center, Cleveland, Ohio

Complex material behavior is represented by a single equation of product form to account for interaction among the various factors. The factors are selected by the physics of the problem and the environment that the model is to represent. For example, different factors will be required for each to represent temperature, moisture, erosion, corrosion, etc. It is important that the equation represent the physics of the behavior in its entirety accurately.

The Multi-Factor Interaction Model (MFIM) is used to evaluate the divot weight (foam weight ejected) from the external launch tanks. The multi-factor has sufficient degrees of freedom to evaluate a large number of factors that may contribute to the divot ejection. It also accommodates all interactions by its product form. Each factor has an exponent that satisfies only two points — the initial and final points. The exponent describes a monotonic path from the initial condition to the final. The exponent values are selected so that the described path makes sense in the absence of experimental data. In the present investigation, the data used were obtained by testing simulated specimens in launching conditions. Re-

sults show that the MFIM is an effective method of describing the divot weight ejected under the conditions investigated.

The problem lies in how to represent the divot weight with a single equation. A unique solution to this problem is a multi-factor equation of product form. Each factor is of the following form $(1 - x_i/x_f)^{e_i}$, where x_i is the initial value, usually at ambient conditions, x_f the final value, and e_i the exponent that makes the curve represented unimodal that meets the initial and final values. The exponents are either evaluated by test data or by technical judgment. A minor disadvantage may be the selection of exponents in the absence of any empirical data. This form has been used successfully in describing the foam ejected in simulated space environmental conditions. Seven factors were required to represent the ejected foam. The exponents were evaluated by least squares method from experimental data.

The equation is used and it can represent multiple factors in other problems as well; for example, evaluation of fatigue life, creep life, fracture toughness, and structural fracture, as well as optimization functions. The software is rather simplistic. Required inputs are initial value, final value, and an exponent for each factor. The number of factors is open-ended. The value is updated as each factor is evaluated. If a factor goes to zero, the previous value is used in the evaluation.

This work was done by Galib H. Abumeri and Christos C. Chamis of Glenn Research Center.

Inquiries concerning rights for the commercial use of this invention should be addressed to NASA Glenn Research Center, Innovative Partnerships Office, Attn: Steve Fedor, Mail Stop 4–8, 21000 Brookpark Road, Cleveland, Ohio 44135. Refer to LEW-18450-1.

Foldable Instrumented Bits for Ultrasonic/Sonic Penetrators

These bits are stowed compactly, then extended to full length when needed.

NASA's Jet Propulsion Laboratory, Pasadena, California

Long tool bits are undergoing development that can be stowed compactly until used as rock- or ground-penetrating probes actuated by ultrasonic/sonic mechanisms. These bits are designed to be folded or rolled into compact form for transport to exploration sites, where they are to be connected to their ultrasonic/sonic actuation mechanisms and unfolded or unrolled to their full lengths for penetrating ground or rock to relatively large depths. These bits can be designed to acquire rock or soil samples and/or to be equipped with sensors for measuring properties of rock or soil *in situ*. These bits can also be designed to be withdrawn from the ground, restowed, and transported for reuse at different exploration sites.

Apparatuses based on the concept of a probe actuated by an ultrasonic/sonic mechanism have been described in numerous prior *NASA Tech Briefs* articles, the most recent and relevant being "Ultrasonic/Sonic Impacting Penetra-tors" (NPO-41666) *NASA Tech Briefs*, Vol. 32, No. 4 (April 2008), page 58. All of those apparatuses are variations on the basic theme of the earliest ones, denoted ultrasonic/sonic drill corers (USDCs). To recapitulate: An apparatus of this type includes a lightweight, low-power, piezoelectrically driven actuator in which ultrasonic and sonic vibrations are generated and coupled to a tool bit. The combination of ultrasonic and sonic vibrations gives rise to a hammering action (and a resulting chiseling action at the tip of the tool bit) that is more effective for drilling than is the microhammering action of ultrasonic vibrations alone. The hammering and chiseling actions are so effective that the size of the axial force needed to make the tool bit advance into soil, rock, or another mate-

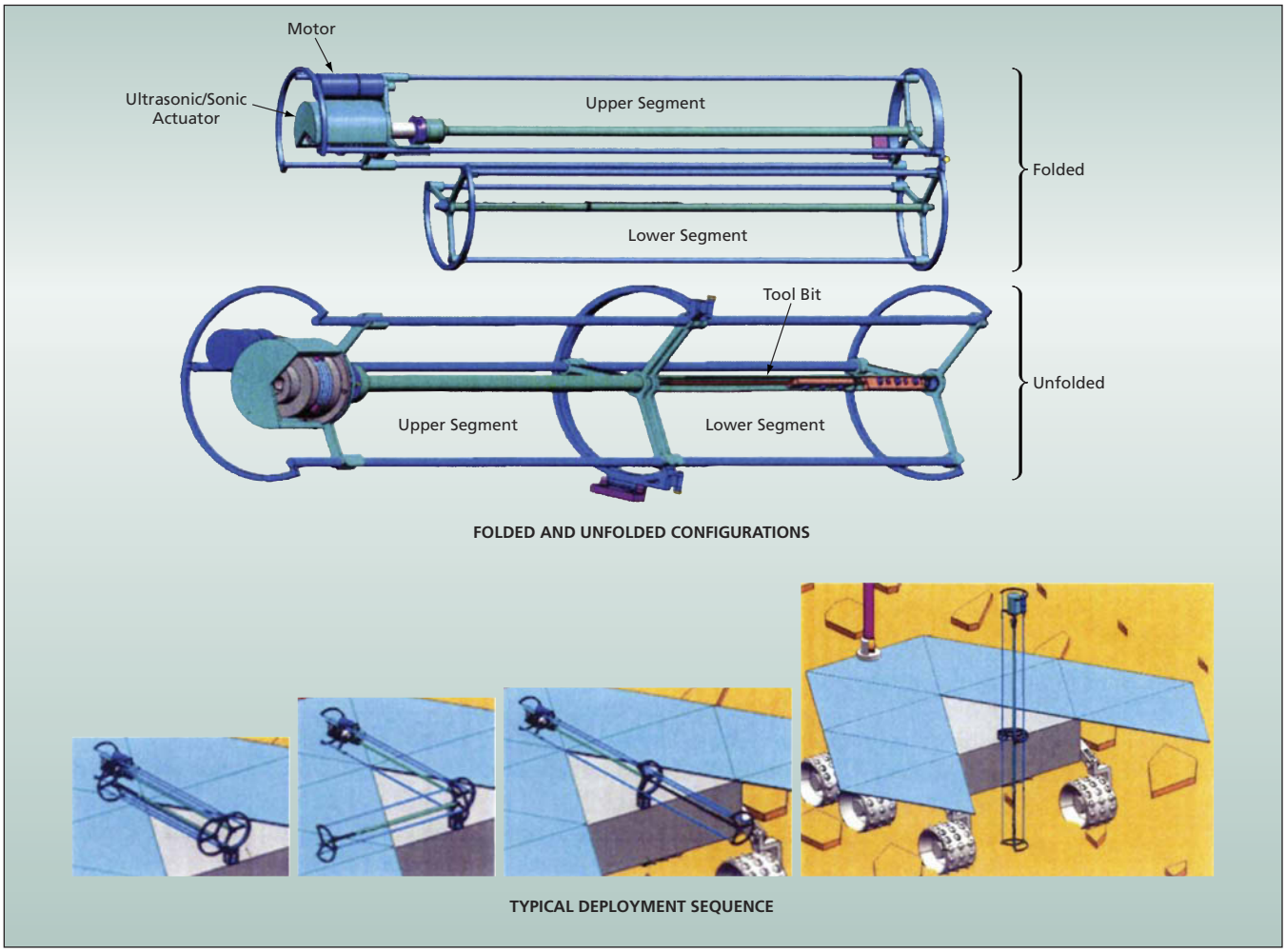

Hinged Lower and Upper Segments of a tool bit and supporting structure are unfolded at the hinges and locked in axial alignment. The resulting assembly is then positioned with the lower end of the tool bit in contact with the ground. The lower views show a conceptual sequence for deployment from an exploratory robotic vehicle, but this sequence is also typical of deployment in other settings.

rial of interest is much smaller than in ordinary twist drilling, ordinary hammering, or ordinary steady pushing.

Examples of properties that could be measured by use of an instrumented tool bit include electrical conductivity, permittivity, magnetic field, magnetic permeability, temperature, and any other properties that can be measured by fiber-optic sensors. The problem of instrumenting a probe of this type is simplified, relative to the problem of attaching electrodes in a rotating drill bit, in two ways:

(1) Unlike a rotating drill bit, a bit of this type does not have flutes, which would compound the problem of ensuring contact between sensors and the side wall of a hole; and (2) there is no need for slip rings for electrical contact between sensor electronic circuitry and external circuitry because, unlike a rotating drill, a tool bit of this type is not rotated continuously during operation.

One design for a tool bit of the present type is a segmented bit with a segmented, hinged support structure (see figure). The bit and its ultrasonic/sonic actuator are supported by a slider/guiding fixture, and its displacement and preload are controlled by a motor. For deployment from the folded configuration, a spring-loaded mechanism rotates the lower segment about the hinges, causing the lower segment to become axially aligned with the upper segment. A latching mechanism then locks the segments of the bit and the corresponding segments of the slider/guiding fixture. Then the entire resulting assembly is maneuvered into position for drilling into the ground.

Another design provides for a bit comprising multiple tubular segments with an inner alignment string, similar to a foldable tent pole comprising multiple tubular segments with an inner elastic cable connecting the two ends. At the beginning of deployment, all segments except the first (lowermost) one remain folded, and the ultrasonic/sonic actuator is clamped to the top of the lowermost segment and used to drive this segment into the ground. When the first segment has penetrated to a specified depth, the second segment is connected to the upper end of the first segment to form a longer rigid tubular bit and the actuator is moved to the upper end of the second segment. The process as described thus far is repeated, adding segments until the desired depth of penetration has been attained.

Yet other designs provide for bits in the form of bistable circular- or rectangular-cross-section tubes that can be stowed compactly like rolls of flat tape and become rigidified upon extension to full length, in a manner partly similar to that of a common steel tape measure. Albeit not marketed for use in tool bits, a bistable reeled composite product that transforms itself from a flat coil to a rigid tube of circular cross section when unrolled, is commercially available under the trade name RolaTube™ and serves as a model for the further development of tool bits of this subtype.

This work was done by Yoseph Bar-Cohen, Mircea Badescu, Theodore Iskenderian, Stewart Sherrit, Xiaoqi Bao, and Randel Lindemann of Caltech for NASA's Jet Propulsion Laboratory. Further information is contained in a TSP (see page 1). ***NPO-45289***

Compact Rare Earth Emitter Hollow Cathode

This rare earth insert for ion and Hall thrusters has longer life and resistance to poisoning.

NASA's Jet Propulsion Laboratory, Pasadena, California

A compact, high-current, hollow cathode utilizing a lanthanum hexaboride (LaB_6) thermionic electron emitter has been developed for use with high-power Hall thrusters and ion thrusters. LaB_6 cathodes are being investigated due to their long life, high current capabilities, and less stringent xenon purity and handling requirements compared to conventional barium oxide (BaO) dispenser cathodes. The new cathode features a much smaller diameter than previously developed versions that permit it to be mounted on axis of a Hall thruster ("internally mounted"), as opposed to the conventional side-mount position external to the outer magnetic circuit ("externally mounted"). The cathode has also been reconfigured to be capable of surviving vibrational loads during launch and is designed to solve the significant heater and materials compatibility problems associated with the use of this emitter material. This has been accomplished in a compact design with the capability of high-emission current (10 to 60 A). The compact, high-current design has a keeper diameter that allows the cathode to be mounted on the centerline of a 6-kW Hall thruster, inside the iron core of the inner electromagnetic coil.

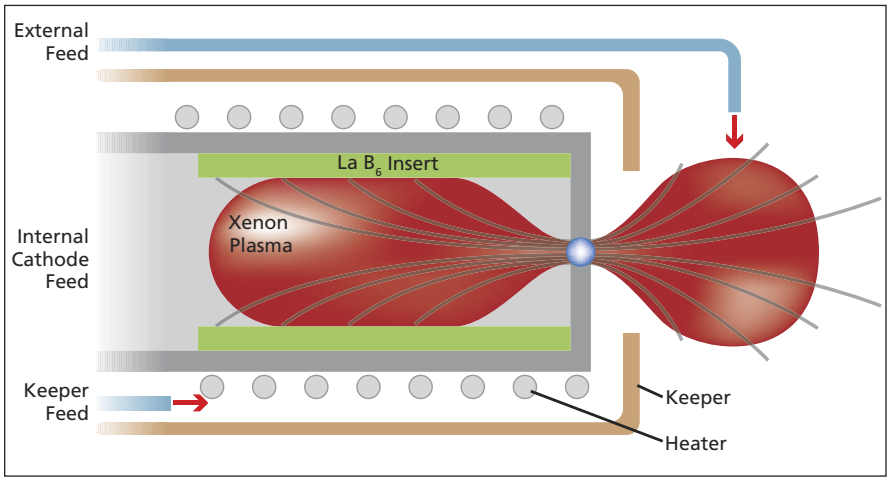

A **Schematic of the Hollow Cathode** with external gas feeds either directly into the cathode plume or into the cathode keeper gap, both of which feed gas into the plasma exterior to the insert region.

Although designed for electric propulsion thrusters in spacecraft station-keeping, orbit transfer, and interplanetary applications, the LaB_6 cathodes are applicable to the plasma processing industry in applications such as optical coatings and semiconductor processing where reactive gases are used. Where current electrical propulsion thrusters with BaO emitters have limited

life and need extremely clean propellant feed systems at a significant cost, these LaB_6 cathodes can run on the crudest-grade xenon propellant available without impact. Moreover, in a laboratory environment, LaB_6 cathodes reduce testing costs because they do not require extended conditioning periods under hard vacuum. Alternative rare earth emitters, such as cerium hexaboride (CeB_6) can be used in this configuration with possibly an even longer emitter life.

This cathode is specifically designed to integrate on the centerline of a high-power Hall thruster, thus eliminating the asymmetries in the plasma discharge common to cathodes previously mounted externally to the thruster's magnetic circuit. An alternative configuration for the cathode uses an external propellant feed. This diverts a fraction of the total cathode flow to an external feed, which can improve the cathode coupling efficiency at lower total mass flow rates. This can improve the overall thruster efficiency, thereby decreasing the required propellant loads for different missions. Depending on the particular mission, reductions in propellant loads can lead to mission enabling capabilities by allowing launch vehicle step-down, greater payload capability, or by extending the life of a spacecraft.

This work was done by Ronald Watkins of Columbus Technologies and Dan Goebel and Richard Hofer of Caltech for NASA's Jet Propulsion Laboratory. Further information is contained in a TSP (see page 1).

High-Precision Shape Control of In-Space Deployable Large Membrane/Thin-Shell Reflectors

Real-time reflector surface figure control uses piezoelectric polymer actuators.

NASA's Jet Propulsion Laboratory, Pasadena, California

This innovation has been developed to improve the resolutions of future space-based active and passive microwave antennas for earth-science remote sensing missions by maintaining surface figure precisions of large membrane/thin-shell reflectors during orbiting. The intention is for these sensing instruments to be deployable at orbit altitudes one or two orders of magnitude higher than Low Earth Orbit (LEO), but still being able to acquire measurements at spatial resolution and sensitivity similar to those of LEO. Because active and passive microwave remote sensors are able to penetrate through clouds to acquire vertical profile measurements of geophysical parameters, it is desirable to elevate them to the higher orbits to obtain orbital geometries that offer large spatial coverage and more frequent observations. This capability is essential for monitoring and for detailed understanding of the life cycles of natural hazards, such as hurricanes, tropical storms, flash floods, and tsunamis.

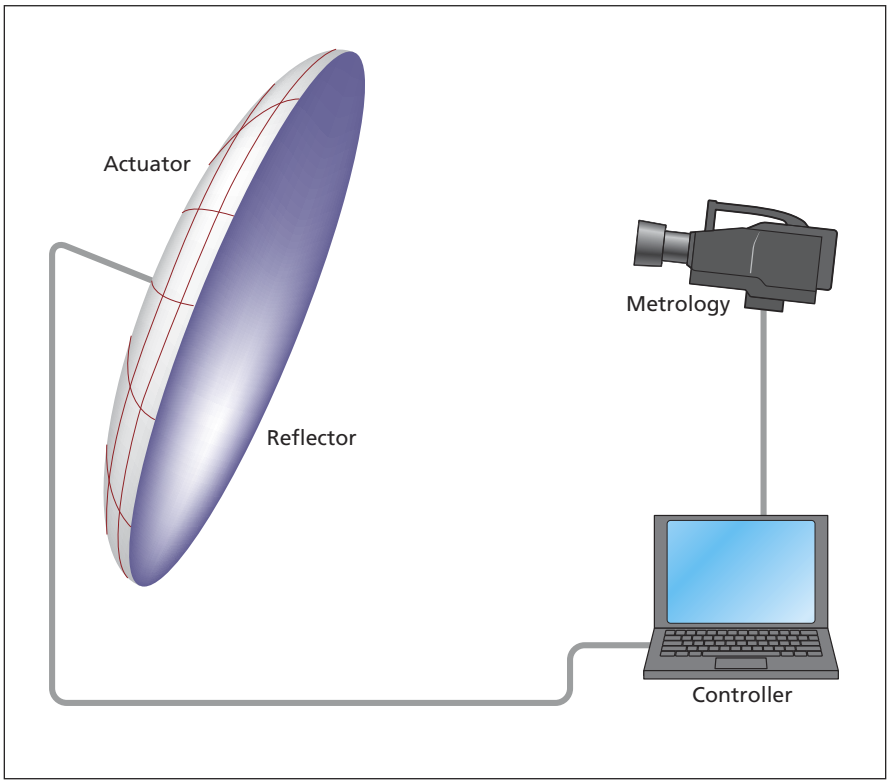

The **Major Components** of the antenna surface control system are illustrated.

Major components of this high-precision antenna-surface-control system include a membrane/thin shell reflector, a metrology sensor, a controller, actuators, and corresponding power amplifier and signal conditioning electronics (see figure). Actuators are attached to the back of the reflector to produce contraction/expansion forces to adjust the shape of the thin-material reflector. The wavefront-sensing metrology system continuously measures the surface figure of the reflector, converts the surface figure to digital data and feeds the data to the controller. The controller determines the control parameters and generates commands to the actuator system. The flexible, piezoelectric polymer actuators are thus activated, providing the control forces needed to correct any distortions that exist in the reflector surface. Piezoelectric polymer actuators are very thin and flexible. They can be implemented on the back of the membrane/thin-shell

reflector without introducing significant amounts of mass or stiffness to the reflector. They can be rolled up or folded to accommodate the packaging needed for launch.

An analytical model of the system, which includes the membrane reflector, actuator, and controller has been developed to investigate the functionality of this control system on a 35-meter-diameter membrane reflector. The performance of this system under external disturbances such as in space thermal loads and W-error due to inflation has been investigated. A subscale breadboard has been developed, and the functionality of this control concept has been demonstrated by this breadboard.

This work was done by Houfei Fang and Eastwood Im of Caltech, and Kon-Well Wang and Qiming Zhang of Penn State University for NASA's Jet Propulsion Laboratory. For more information, contact iaoffice@jpl.nasa.gov. NPO-44913

Rapid Active Sampling Package

A field-deployable, battery-operated tool enables rock sampling in the field.

NASA's Jet Propulsion Laboratory, Pasadena, California

A field-deployable, battery-powered Rapid Active Sampling Package (RASP), originally designed for sampling strong materials during lunar and planetary missions, shows strong utility for terrestrial geological use. The technology is proving to be simple and effective for sampling and processing materials of strength. Although this originally was intended for planetary and lunar applications, the RASP is very useful as a powered hand tool for geologists and the mining industry to quickly sample and process rocks in the field on Earth.

The RASP allows geologists to surgically acquire samples of rock for later laboratory analysis. This tool, roughly the size of a wrench, allows the user to cut away swaths of weathering rinds, revealing pristine rock surfaces for observation and subsequent sampling with the same tool. RASPing deeper (≈3–5 cm) exposes single rock strata *in-situ*. Where a geologist's hammer can only expose unweathered layers of rock, the RASP can do the same, and then has the added ability to capture and process samples into powder with particle sizes less than 150 microns, making it easier for XRD/XRF (x-ray diffraction/x-ray fluorescence). The tool uses a rotating rasp bit (or two counter-rotating bits) that resides inside or above the catch container. The container has an open slot to allow the bit to extend outside the container and to allow cuttings to enter and be caught. When the slot and rasp bit are in contact with a substrate, the bit is plunged into it in a matter of seconds to reach pristine rock.

A user in the field may sample a rock multiple times at multiple depths in minutes, instead of having to cut out huge, heavy rock samples for transport back to a lab for analysis. Because of the speed and accuracy of the RASP, hundreds of samples can be taken in one day. RASP-acquired samples are small and easily carried. A user can characterize more area in less time than by using conventional methods. The field-deployable RASP used a Ni/Cad rechargeable battery. Power usage was less than 1 W-h/cm^3 even when sampling strong basalts, so many samples could be taken on a single battery charge.

The prototype field RASP was equipped with a load tube in which sealable sample containers were inserted. Positioning the tool upside-down conveniently loaded the sample containers with powdered rock samples. This technology could be adapted to existing battery-operated rotary tools, or could be used as a stand-alone sampling tool.

This work was done by Gregory Peters of Caltech for NASA's Jet Propulsion Laboratory. For more information, contact iaoffice@jpl.nasa.gov. NPO-44946

Miniature Lightweight Ion Pump

This lightweight pump with no moving parts eliminates the need for a backup pump.

NASA's Jet Propulsion Laboratory, Pasadena, California

This design offers a larger surface area for pumping of active gases and reduces the mass of the pump by eliminating the additional vacuum enclosure. There are three main components to this ion pump: the cathode and anode pumping elements assembly, the vacuum enclosure (made completely of titanium and used as the cathode and maintained at ground potential) containing the assembly, and the external magnet. These components are generally put in a noble diode (or differential) configuration of the ion pump technology. In the present state of the art, there are two cathodes, one made of titanium and the other of tantalum. The anodes are made up of an array of stainless steel cylinders positioned between the two cathodes.

All the elements of the pump are in a vacuum enclosure. After the reduction of pressure in this enclosure to a few microns, a voltage is applied between the cathode and the anode elements. Electrons generated by the ionization are accelerated toward the anodes that are confined in the anode space by the axial magnetic field. For the generation of the axial field along the anode elements, the magnet is designed in a C-configuration and is fabricated from rare earth magnetic materials (Nd-B-Fe or Sm-Co) possessing high energy product values, and the yoke is fabricated from the high permeability material (Hiperco-50A composed of Fe-Co-V). The electrons in this region collide with the gas molecules and generate their positive ions. These ions are accelerated into the cathode and eject cathode material (Ti). The neutral atoms deposit on the anode surfaces. Because of the chemical activity of

Ti, the atoms combine with chemically active gas molecules (e.g. N_2, O_2, etc.) and remove them. New layers of Ti are continually deposited, and the pumping of active gases is thus accomplished.

Pumping of the inert gases is accomplished by their burial several atomic layers deep into the cathode. However, they tend to re-emit if the entrapping lattice atoms are sputtered away. For stable pumping of inert gases, one side of the cathode is made of Ta. Impaction on Ta produces energetic, neutral atoms that pump the inert gases on the anode structure at the peripheral areas of the cathodes (between anode rings). For inert gases stability, a post design has been implemented. Here, posts of cathode material (Ti) are mounted on the cathode. These protrude into the initial part of the anode elements. Materials sputtered from the posts condense on the anode assembly and on the cathode plane at higher rates than in the normal diodes due to enhanced sputtering at glancing angles from geometrical considerations. This increases pumping by burial. This post design has enhanced pumping rates for both active and inert gases, compared with conventional designs.

This work was done by Mahadeva P. Sinha of Caltech for NASA's Jet Propulsion Laboratory.

In accordance with Public Law 96-517, the contractor has elected to retain title to this invention. Inquiries concerning rights for its commercial use should be addressed to:

Innovative Technology Assets Management
JPL
Mail Stop 202-233
4800 Oak Grove Drive
Pasadena, CA 91109-8099
E-mail: iaoffice@jpl.nasa.gov

Refer to NPO-30628, volume and number of this NASA Tech Briefs *issue, and the page number.*

Cryogenic Transport of High-Pressure-System Recharge Gas

Advantages include low pressure and high density during transport.

Lyndon B. Johnson Space Center, Houston, Texas

A method of relatively safe, compact, efficient recharging of a high-pressure room-temperature gas supply has been proposed. In this method, the gas would be liquefied at the source for transport as a cryogenic fluid at or slightly above atmospheric pressure. Upon reaching the destination, a simple heating/expansion process would be used to (1) convert the transported cryogenic fluid to the room-temperature, high-pressure gaseous form in which it is intended to be utilized and (2) transfer the resulting gas to the storage tank of the system to be recharged.

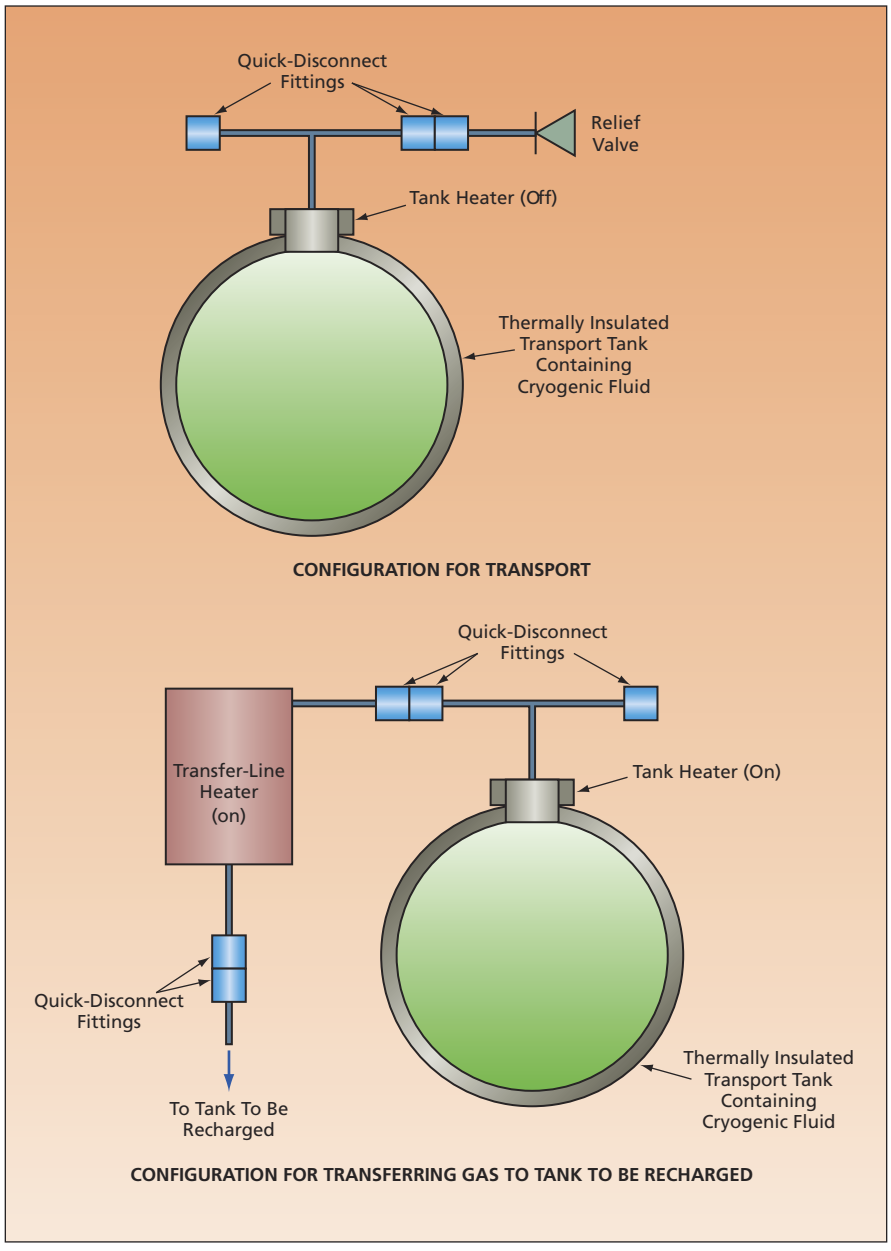

An **Insulated Transport Tank** would contain a cryogenic fluid, which would be warmed to convert it to a pressurized gas.

In conventional practice for recharging high-pressure-gas systems, gases are transported at room temperature in high-pressure tanks. For recharging a given system to a specified pressure, a transport tank must contain the recharge gas at a much higher pressure. At the destination, the transport tank is connected to the system storage tank to be recharged, and the pressures in the transport tank and the system storage tank are allowed to equalize. One major disadvantage of the conventional approach is that the high transport pressure poses a hazard. Another disadvantage is the waste of a significant amount of recharge gas. Because the transport tank is disconnected from the system storage tank when it is at the specified system recharge pressure, the transport tank still contains a significant amount of recharge gas (typically on the order of half of the amount transported) that cannot be used.

In the proposed method, the cryogenic fluid would be transported in a suitably thermally insulated tank that would be capable of withstanding the recharge pressure of the destination tank. The tank would be equipped with quick-disconnect fluid-transfer fittings and with a low-power electric heater (which would not be used during transport). In preparation for transport, a relief valve would be attached via one of the quick-disconnect fittings (see figure). During transport, the interior of the tank would be kept at a near-ambient pressure — far below the recharge pressure. As leakage of heat into the tank caused vaporization of the cryogenic fluid, the resulting gas would be vented through the relief valve, which would be set to maintain the pressure in the tank at the transport value. Inasmuch as the density of a cryogenic fluid at atmospheric pressure greatly exceeds that of the corresponding gas in a practical high-pressure tank at room temperature, a tank for transporting a given mass of gas according to the proposed method could be

smaller (and, hence, less massive) than is a tank needed for transporting the same mass of gas according to the conventional method.

Upon arrival at the destination, the transport tank would be connected to the tank to be recharged via a transfer line that would include a second low-power electric heater. The relief valve would be disconnected and the line to the gas system opened, causing the pressure in the transport tank to rise to the system pressure. The transport tank and transfer-line electric heaters would be turned on, causing the contents of the tank to expand under high pressure and flow out through the transfer line. The transfer-line heater would further warm the flowing fluid to room temperature. The relative power levels of the electric heaters would be set to ensure that the fluid expelled from the tank by the tank heater could be delivered as room-temperature gas to the tank to be recharged. The transfer of gas would be complete once the remaining gas inside the transport tank had been heated to room temperature. By virtue of the difference between densities, at completion, the majority of the mass of the transported cryogenic fluid would have been converted to gas and transferred to the recharged tank.

This work was done by Eugene K. Ungar and Warren P. Ruemmele of Johnson Space Center and William Carl Bohannon of The Boeing Co. Further information is contained in a TSP (see page 1). MSC-24343-1

Water-Vapor Raman Lidar System Reaches Higher Altitude

Signal-to-noise ratios are increased over those of prior such systems.

NASA's Jet Propulsion Laboratory, Pasadena, California

A Raman lidar system for measuring the vertical distribution of water vapor in the atmosphere is located at the Table Mountain Facility (TMF) in California. Raman lidar systems for obtaining vertical water-vapor profiles in the troposphere have been in use for some time. The TMF system incorporates a number of improvements over prior such systems that enable extension of the altitude range of measurements through the tropopause into the lower stratosphere.

One major obstacle to extension of the altitude range is the fact that the mixing ratio of water vapor in the tropopause and the lower stratosphere is so low that Raman lidar measurements in this region are limited by noise. Therefore, the design of the TMF system incorporates several features intended to maximize the signal-to-noise ratio. These features include (1) the use of 355-nm-wavelength laser pulses having an energy (0.9 J per pulse) that is high relative to the laser-pulse energy levels of prior such systems, (2) a telescope having a large aperture (91 cm in diameter) and a narrow field of view (angular width ≈0.6 mrad), and (3) narrow-bandpass (wavelength bandwidth 0.6 nm) filters for the water-vapor Raman spectral channels. In addition to the large-aperture telescope, three telescopes having apertures 7.5 cm in diameter are used to collect returns from low altitudes.

The receiver portion of this lidar system has a total of eight channels (see figure). These include three channels for the water-vapor Raman returns at a wavelength of 407 nm, three channels for the nitrogen Raman returns at a wavelength of 387 nm, and two channels for elastic-scattering returns at the laser wavelength of 355 nm. Three of the channels (a 387-, a 407-, and a 355-nm channel), denoted the near channels, process the Raman and elastic returns collected by the three smaller telescopes. The remaining five channels, denoted the far channels, process the Raman and elastic returns collected by the large telescope. The elastic-scattering returns are used primarily for deriving temperature profiles. The light in each channel is measured by use of a photomultiplier tube, the output of which is fed to a commercially available optical-transient recorder operating as a photon-counting multichannel scaler. The altitude interval of each bin of the scaler is 7.5 m, but typically, bins are summed together in groups of 10, yielding discretization of altitude in increments of 75 m.

The light collected by the large telescope is focused into an optical fiber, which delivers the light to a lens that

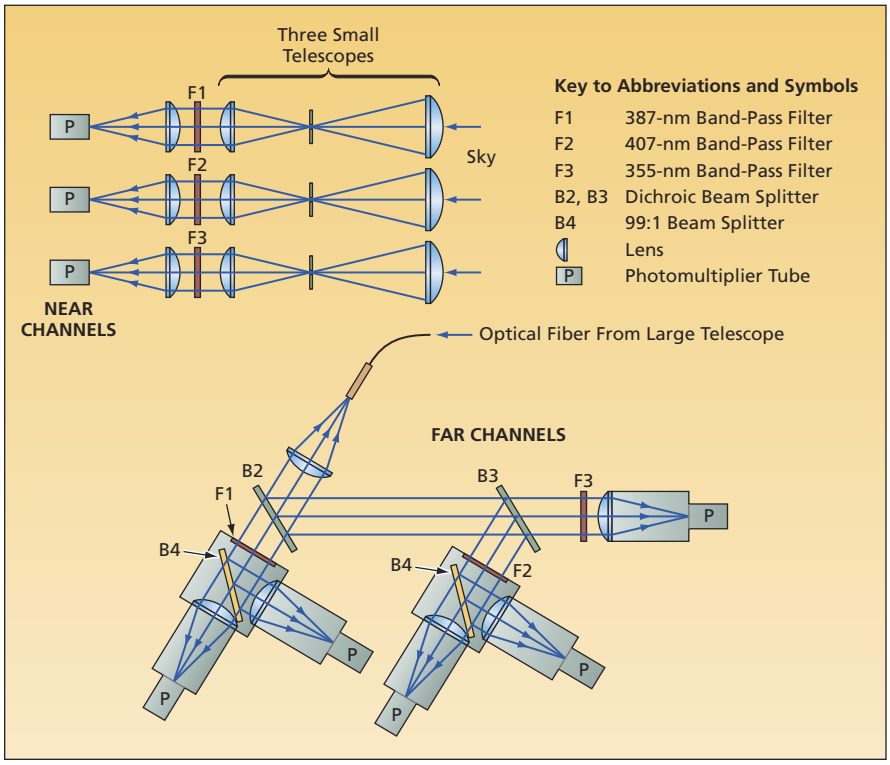

These Partly Schematic Optical Layouts show the paths followed by Raman and elastically scattered returns collected by a large telescope and three smaller telescopes.

collimates the light into a series of beam splitters. Among the beam splitters are a 99:1 beam splitter for each of the two Raman wavelength bands. In addition to extending the dynamic range of the photon counting system, this arrangement enables better corrections for pulse pile-up saturation effects than could otherwise be made. The arrangement is such as to make the 387- and 407-mm Raman signals in the large-telescope 1-percent splitter outputs approximately equal in magnitude to the corresponding signals from the smaller telescopes; this makes it possible to use the signals from the small telescopes to correct for effects of overlap of photon pulses in signals from the large telescope collected from low altitudes.

This work was done by Thierry Leblanc and I. Stewart McDermid of Caltech for NASA's Jet Propulsion Laboratory. Further information is contained in a TSP (see page 1). NPO-45007

Compact Ku-Band T/R Module for High-Resolution Radar Imaging of Cold Land Processes

This module can be used in phased-array antennas for radar or communications.

NASA's Jet Propulsion Laboratory, Pasadena, California

Global measurement of terrestrial snow cover is critical to two of the NASA Earth Science focus areas: (1) climate variability and change and (2) water and energy cycle. For radar backscatter measurements, Ku-band frequencies, scattered mainly within the volume of the snowpack, are most suitable for the SWE (snow-water equivalent) measurements. To isolate the complex effects of different snowpack (density and snow-grain size), and underlying soil properties and to distinctly determine SWE, the space-based synthetic aperture radar (SAR) system will require a dual-frequency (13.4 and 17.2 GHz) and dual-polarization approach.

A transmit/receive (T/R) module was developed operating at Ku-band frequencies to enable the use of active electronic scanning phased-array antenna for wide-swath, high-resolution SAR imaging of terrestrial snow cover. The T/R module has an integrated calibrator, which compensates for all environmental- and time-related changes, and results in very stable power and amplitude characteristics. The module was designed to operate over the full frequency range of 13 to 18 GHz, although only the two frequencies, 13.4 GHz and 17.2 GHz, will be used in this SAR radar application. Each channel of the transmit module produces >4 W (35 dbm) over the operating bandwidth of 20 MHz. The stability requirements of <0.1 dB receive gain accuracy and <0.1 dB transmit power accuracy over a wide temperature range are achieved using a self-correction scheme, which does real-time amplitude calibration so that the module characteristics are continually corrected. All the calibration circuits are within the T/R module.

The timing and calibration sequence is stored in a control FPGA (field-programmable gate array) while an internal 128K×8bit high-speed RAM (random access memory) stores all the calibration values. The module was designed using advanced components and packaging techniques to achieve integration of the electronics in a 2×6.5×1-in. (5×17×2.5-cm) package. The module size allows 4 T/R modules to feed the 16×16-element subarray on an antenna panel. The T/R module contains four transmit channels and eight receive channels (horizontal and vertical polarizations). Each channel contains GaAs MMIC (monolithic microwave integrated circuit) amplifiers, a 5-bit phase shifter, and a programmable

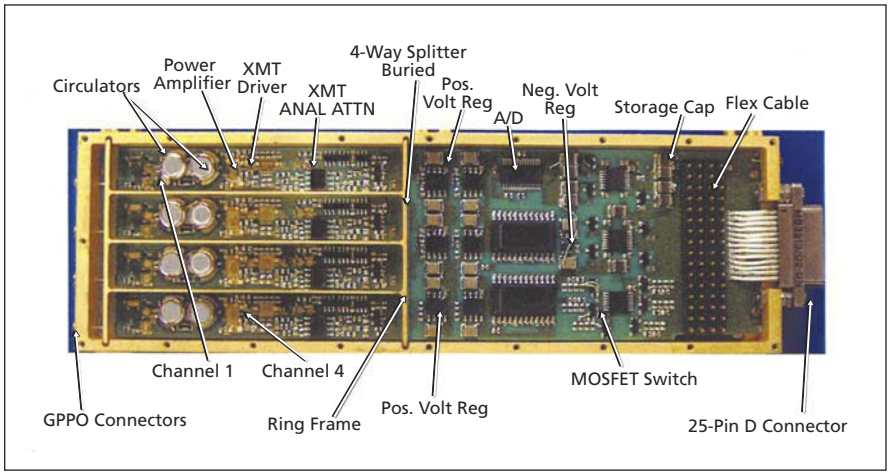

Figure 1 **Transmission Side of the T/R Module** showing the components.

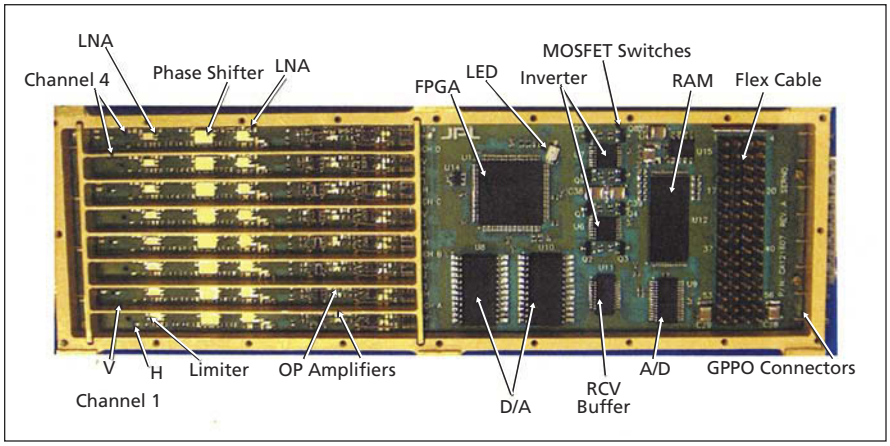

Figure 2. **Receiving Side of the T/R Module** showing the components.

attenuator. To meet the compact size and maintain isolation between the channels, a two-sided module approach was adapted. The transmit side of the module houses the four transmit channels, the control FPGA, and the power regulators and logic circuitry. It also contains the 4-way stripline power splitter. The 4-dual channel receivers are packaged on the reverse side of the module along with the horizontal and vertical power combiners, and some logic and power conditioning circuits. The transmit and receive sides of the T/R module with the component identifications are shown in Figures 1 and 2.

The broadband, 4-channel, highly stable self calibrating T/R module is a useful building block for other radar and communication phased-array systems operating in this band.

This work was done by Constantine Andricos, Simon H. Yueh, Vladimir A. Krimskiy, of Caltech and Yahya Rahmat-Samii of UCLA for NASA's Jet Propulsion Laboratory. For more information, contact iaoffice@jpl.nasa.gov. NPO-46428

Wide-Field-of-View, High-Resolution, Stereoscopic Imager

Lyndon B. Johnson Space Center, Houston, Texas

A device combines video feeds from multiple cameras to provide wide-field-of-view, high-resolution, stereoscopic video to the user. The prototype under development consists of two camera assemblies, one for each eye. One of these assemblies incorporates a mounting structure with multiple cameras attached at offset angles. The video signals from the cameras are fed to a central processing platform where each frame is color processed and mapped into a single contiguous wide-field-of-view image.

Because the resolution of most display devices is typically smaller than the processed map, a cropped portion of the video feed is output to the display device. The positioning of the cropped window will likely be controlled through the use of a head tracking device, allowing the user to turn his or her head side-to-side or up and down to view different portions of the captured image. There are multiple options for the display of the stereoscopic image. The use of head mounted displays is one likely implementation. However, the use of 3D projection technologies is another potential technology under consideration,

The technology can be adapted in a multitude of ways. The computing platform is scalable, such that the number, resolution, and sensitivity of the cameras can be leveraged to improve image resolution and field of view. Miniaturization efforts can be pursued to shrink the package down for better mobility. Power savings studies can be performed to enable unattended, remote sensing packages. Image compression and transmission technologies can be incorporated to enable an improved telepresence experience.

This work was done by Eric F. Prechtl of Axis Engineering Technologies, Inc., and Raymond J. Sedwick of the Massachusetts Institute of Technology for Johnson Space Center. For further information, contact the JSC Innovation Partnerships Office at (281) 483-3809.

In accordance with Public Law 96-517, the contractor has elected to retain title to this invention. Inquiries concerning rights for its commercial use should be addressed to:

Axis Engineering Technologies, Inc.
One Broadway, 14th Floor
Cambridge, MA 02142
Phone No.: (617) 225-4414
Fax No.: (617) 225-4439
E-mail: eric@axisetech.com

Refer to MSC-23977-1, volume and number of this NASA Tech Briefs *issue, and the page number.*

Electrical Capacitance Volume Tomography With High-Contrast Dielectrics

This nondestructive evaluation tool finds fluid levels in nonconducting composite materials.

John F. Kennedy Space Center, Florida

The Electrical Capacitance Volume Tomography (ECVT) system has been designed to complement the tools created to sense the presence of water in nonconductive spacecraft materials, by helping to not only find the approximate location of moisture but also its quantity and depth.

The ECVT system has been created for use with a new image reconstruction algorithm capable of imaging high-contrast dielectric distributions. Rather than relying solely on mutual capacitance readings as is done in traditional electrical capacitance tomography applications, this method reconstructs high-resolution images using only the self-capacitance measurements. The image reconstruction method assumes that the material under inspection consists of a binary dielectric distribution, with either a high relative dielectric value representing the water or a low dielectric value for the background material. By constraining the unknown dielectric material to one of two values, the inverse math problem that must be solved to generate the image is no longer ill-determined. The image resolution becomes limited only by the accuracy and resolution of the measurement circuitry. Images were reconstructed using this method with both synthetic and real data acquired using an aluminum structure inserted at different positions within the sensing region.

The cuboid geometry of the system has two parallel planes of 16 conductors arranged in a 4×4 pattern. The electrode geometry consists of parallel planes of copper conductors, connected through custom-built switch electronics, to a commercially available capacitance to digital converter. The figure shows

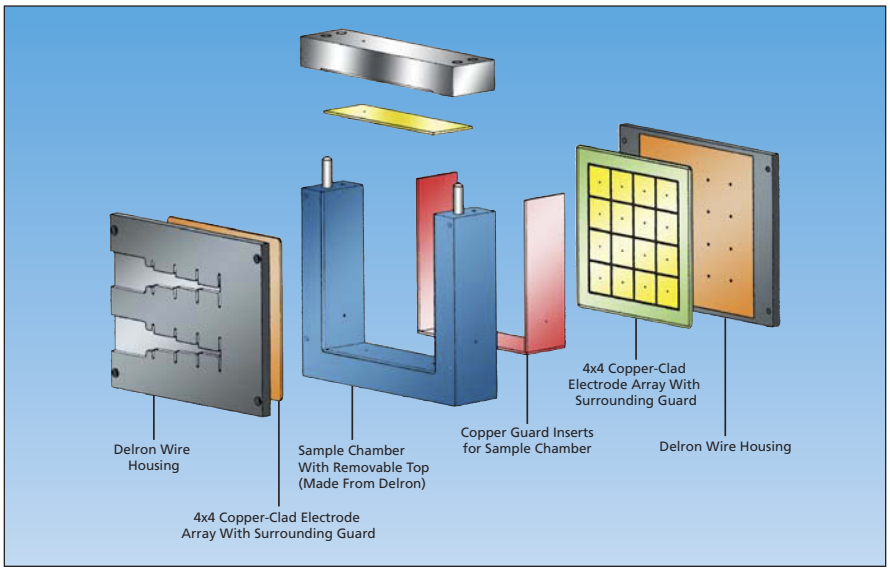

An exploded view of the **ECVT Sensor** shows the face of one of the two 4×4 arrays of conductors. Each sensing element is 1.9 cm on a side, placed on 2-cm centers, and separated from the opposing array by 3.3 cm.

two 4×4 arrays of electrodes milled from square sections of copper-clad circuitboard material and mounted on two pieces of glass-filled plastic backing, which were cut to approximately square shapes, 10 cm on a side. Each electrode is placed on 2.0-cm centers. The parallel arrays were mounted with the electrode arrays approximately 3 cm apart. The open ends were surrounded by a metal guard to reduce the sensitivity of the electrodes to outside interference and to help maintain the spacing between the arrays.

Other uses for this innovation potentially include quantifying the amount of commodity remaining in the fuel and oxidizer tanks while on-orbit without having to fire spacecraft engines. Another orbit application is moisture sensing in plant-growth experiments because microgravity causes moisture in soil to distribute itself in unusual ways.

At the moment, the hardware and image reconstruction technique may only be of interest to people involved in nondestructive evaluation. The reconstructed image takes almost a full week to reproduce with existing computer power. However, because computer power and speeds follows Moore's Law, execution times are likely to become acceptable within the next five to eight years. The code was written in Mathematica for dedicated use with the ECVT system. In its present form, it is not suitable to be used directly as a consumer product. However, the code could be likely improved by rewriting it in a compiled language such as C or Fortran.

This work was done by Mark Nurge of Kennedy Space Center. KSC-13038

Wavefront Control and Image Restoration With Less Computing

There are numerous potential applications in scientific, medical, and military imaging.

Goddard Space Flight Center, Greenbelt, Maryland

PseudoDiversity is a method of recovering the wavefront in a sparse- or segmented-aperture optical system typified by an interferometer or a telescope equipped with an adaptive primary mirror consisting of controllably slightly moveable segments. (PseudoDiversity should not be confused with a radio-antenna-arraying method called "pseudo-diversity".) As in the cases of other wavefront-recovery methods, the streams of wavefront data generated by means of PseudoDiversity are used as feedback signals for controlling electromechanical actuators of the various segments so as to correct wavefront errors and thereby, for example, obtain a clearer, steadier image of a distant object in the presence of atmospheric turbulence. There are numerous potential applications in astronomy, remote sensing from aircraft and spacecraft, targeting missiles, sighting military targets, and medical imaging (including microscopy) through such intervening media as cells or water.

In comparison with prior wavefront-recovery methods used in adaptive optics, PseudoDiversity involves considerably simpler equipment and procedures and less computation.

For PseudoDiversity, there is no need to install separate metrological equipment or to use any optomechanical components beyond those that are already parts of the optical system to which the method is applied. In PseudoDiversity, the actuators of a subset of the segments or subapertures are driven to make the segments dither in the piston, tilt, and tip degrees of freedom. Each aperture is dithered at a unique frequency at an amplitude of a half wavelength of light.

During the dithering, images on the focal plane are detected and digitized at a rate of at least four samples per dither period. In the processing of the image samples, the use of different dither frequencies makes it possible to determine the separate effects of the various dithered segments or apertures. The digitized image-detector outputs are processed in the spatial-frequency (Fourier-transform) domain to obtain measures of the piston, tip, and tilt errors over each segment or subaperture. Once these measures are known, they are fed back to the actuators to correct the errors. In addition, measures of errors that remain after correction by use of the actuators are further utilized in an algorithm in which the image is phase-corrected in the spatial-frequency domain and then transformed back to the spatial domain at each time step and summed with the images from all previous time steps to obtain a final image having a greater signal-to-noise ratio (and, hence, a visual quality) higher than would otherwise be attainable.

This work was done by Richard G. Lyon of Goddard Space Flight Center. Further information is contained in a TSP (see page 1). GSC-15464-1

Polarization Imaging Apparatus

Lyndon B. Johnson Space Center, Houston, Texas

A polarization imaging apparatus has shown promise as a prototype of instruments for medical imaging with contrast greater than that achievable by use of non-polarized light. The underlying principles of design and operation are derived from observations that light interacts with tissue ultrastructures that affect reflectance, scattering, absorption, and polarization of light. The apparatus utilizes high-speed electro-optical components for generating light properties and acquiring polarization images through aligned polarizers. These components include phase retarders made of OptoCeramic® material — a ceramic that has a high electro-optical coefficient.

The apparatus includes a computer running a program that implements a novel algorithm for controlling the phase retarders, capturing image data, and computing the Stokes polarization images. Potential applications include imaging of superficial cancers and other skin lesions, early detection of diseased cells, and microscopic analysis of tissues. The high imaging speed of this apparatus could be beneficial for observing live cells or tissues, and could enable rapid identification of moving targets in astronomy and national defense. The apparatus could also be used as an analysis tool in material research and industrial processing.

This work was done by Yingyin K. Zou and Qiushui Chen of Boston Applied Technologies, Inc. for Johnson Space Center. For further information, contact the JSC Innovation Partnerships Office at (281) 483-3809.

In accordance with Public Law 96-517, the contractor has elected to retain title to this invention. Inquiries concerning rights for its commercial use should be addressed to:

Boston Applied Technologies
6F Gill Street
Woburn, MA 01801
Phone No.: (781) 935-2800

Refer to MSC-24173-1, volume and number of this NASA Tech Briefs *issue, and the page number.*

Stereoscopic Machine-Vision System Using Projected Circles

This system identifies obstacles in relatively short processing times.

John H. Glenn Research Center, Cleveland, Ohio

A machine-vision system capable of detecting obstacles large enough to damage or trap a robotic vehicle is undergoing development. The system includes (1) a pattern generator that projects concentric circles of laser light forward onto the terrain, (2) a stereoscopic pair of cameras that are aimed forward to acquire images of the circles, (3) a frame grabber and digitizer for acquiring image data from the cameras, and (4) a single-board computer that processes the data. The system is being developed as a prototype of machine-vision systems to enable robotic vehicles ("rovers") on remote planets to avoid craters, large rocks, and other terrain features that could capture or damage the vehicles. Potential terrestrial applications of systems like this one could include terrain mapping, collision avoidance, navigation of robotic vehicles, mining, and robotic rescue.

This system is based partly on the same principles as those of a prior stereoscopic machine-vision system in which the cameras acquire images of a single stripe of laser light that is swept forward across the terrain. However, this system is designed to afford improvements over some of the undesirable features of the prior system, including the need for a pan-and-tilt mechanism to aim the laser to generate the swept stripe, ambiguities in interpretation of the single-stripe image, the time needed to sweep the stripe across the terrain and process the data from many images acquired during that time, and difficulty of calibration because of the narrowness of the stripe.

In this system, the pattern generator does not contain any moving parts and need not be mounted on a pan-and-tilt

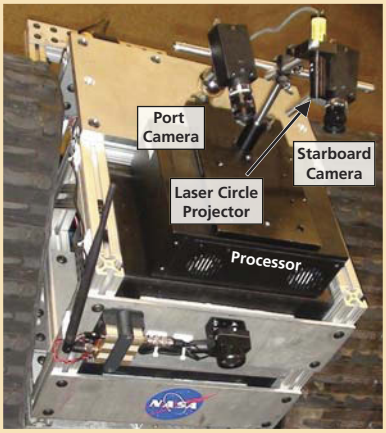

Vision System

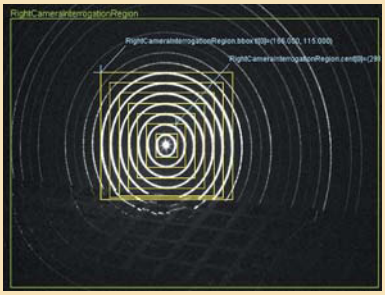

IMAGE IN LEFT CAMERA
LOOKING 10° LEFT OVER A CLIFF

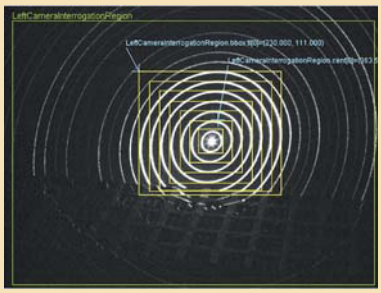

IMAGE IN RIGHT CAMERA
LOOKING 10° LEFT OVER A CLIFF

Concentric Circles of Light are projected forward and observed by a stereoscopic pair of cameras. Distortions of the circle images in the cameras are used to identify and locate objects large enough to constitute obstacles.

mechanism: the pattern of concentric circles is projected steadily in the forward direction. The system calibrates itself by use of data acquired during projection of the concentric-circle pattern onto a known target representing flat ground. The calibration-target image data are stored in the computer memory for use as a template in processing terrain images.

During operation on terrain, the images acquired by the left and right cameras are analyzed. The analysis includes (1) computation of the horizontal and vertical dimensions and the aspect ratios of rectangles that bound the circle images and (2) comparison of these aspect ratios with those of the template. Coordinates of distortions of the circles are used to identify and locate objects. If the analysis leads to identification of an object of significant size, then stereoscopic-vision algorithms are used to estimate the distance to the object. The time taken in performing this analysis on a single pair of images acquired by the left and right cameras in this system is a fraction of the time taken in processing the many pairs of images acquired in a sweep of the laser stripe across the field of view in the prior system.

The results of the analysis include data on sizes and shapes of, and distances and directions to, objects. Coordinates of objects are updated as the vehicle moves so that intelligent decisions regarding speed and direction can be made. The results of the analysis are utilized in a computational decision-making process that generates obstacle-avoidance data and feeds those data to the control system of the robotic vehicle.

This work was done by Jeffrey R. Mackey of ASRC Aerospace Corp. for Glenn Research Center. Further information is contained in a TSP (see page 1).

Inquiries concerning rights for the commercial use of this invention should be addressed to NASA Glenn Research Center, Innovative Partnerships Office, Attn: Steve Fedor, Mail Stop 4–8, 21000 Brookpark Road, Cleveland, Ohio 44135. Refer to LEW-18320-1

Metal Vapor Arcing Risk Assessment Tool

Lyndon B. Johnson Space Center, Houston, Texas

The Tin Whisker Metal Vapor Arcing Risk Assessment Tool has been designed to evaluate the risk of metal vapor arcing and to help facilitate a decision toward a researched risk disposition. Users can evaluate a system without having to open up the hardware. This process allows for investigating components at risk rather than spending time and money analyzing every component. The tool points to a risk level and provides direction for appropriate action and documentation.

This process was written by Monika C. Hill of The Boeing Company and Henning W. Leidecker of Goddard Space Flight Center for Johnson Space Center.

Title to this invention has been waived under the provisions of the National Aeronautics and Space Act {42 U.S.C. 2457(f)}, to The Boeing Company. Inquiries concerning licenses for its commercial development should be addressed to:

Boeing Licensing Professional,
Terrance Mason
E-mail : terrance.mason@boeing.com
Phone No.: (562) 797-9034.
Reference Boeing Docket No. 06-0756.

Refer to MSC-24300, volume and number of this NASA Tech Briefs *issue, and the page number.*

Performance Bounds on Two Concatenated, Interleaved Codes

It is now possible to calculate tight bounds at high SNR.

NASA's Jet Propulsion Laboratory, Pasadena, California

A method has been developed of computing bounds on the performance of a code comprised of two linear binary codes generated by two encoders serially concatenated through an interleaver. Originally intended for use in evaluating the performances of some codes proposed for deep-space communication links, the method can also be used in evaluating the performances of short-block-length codes in other applications.

The method applies, more specifically, to a communication system in which following processes take place:

- At the transmitter, the original binary information that one seeks to transmit is first processed by an encoder into an outer code (C_o) characterized by, among other things, a pair of numbers (n,k), where n $(n > k)$ is the total number of code bits associated with k information bits and $n–k$ bits are used for correcting or at least detecting errors. Next, the outer code is processed through either a block or a convolutional interleaver. In the block interleaver, the words of the outer code are processed in blocks of I words. In the convolutional interleaver, the interleaving operation is performed bit-wise in N rows with delays that are multiples of B bits. The output of the interleaver is processed through a second encoder to obtain an inner code (C_i) characterized by (n_i,k_i).
- The output of the inner code is transmitted over an additive-white-Gaussian- noise channel characterized by a symbol signal-to-noise ratio (SNR) E_s/N_o and a bit SNR E_b/N_o.
- At the receiver, an inner decoder generates estimates of bits. Depending on whether a block or a convolutional interleaver is used at the transmitter, the sequence of estimated bits is processed through a block or a convolutional de-interleaver, respectively, to obtain estimates of code words. Then the estimates of the code words are processed through an outer decoder, which generates estimates of the original information along with flags indicating which estimates are presumed to be correct and which are found to be erroneous.

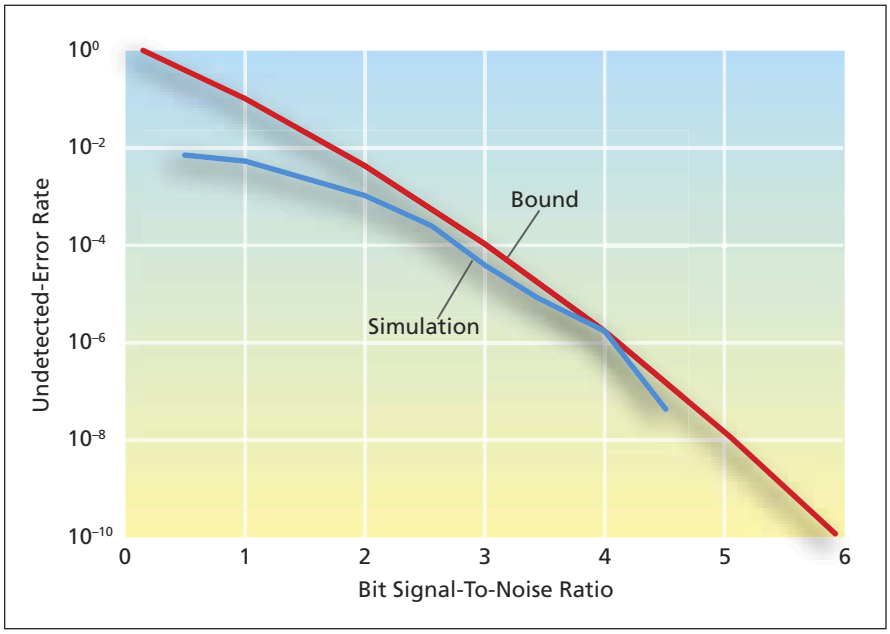

The **Undetected-Error Rate** of one of the coding/decoding communication systems studied in this research was determined by computational simulation and is compared here with the upper bound on the undetected-error rate calculated by the present method.

From the perspective of the present method, the topic of major interest is the

performance of the communication system as quantified in the word-error rate and the undetected-error rate as functions of the SNRs and the total latency of the interleaver and inner code. The method is embodied in equations that describe bounds on these functions. Throughout the derivation of the equations that embody the method, it is assumed that the decoder for the outer code corrects any error pattern of t or fewer errors, detects any error pattern of s or fewer errors, may detect some error patterns of more than s errors, and does not correct any patterns of more than t errors. Because a mathematically complete description of the equations that embody the method and of the derivation of the equations would greatly exceed the space available for this article, it must suffice to summarize by reporting that the derivation includes consideration of several complex issues, including relationships between latency and memory requirements for block and convolutional codes, burst error statistics, enumeration of error-event intersections, and effects of different interleaving depths.

In a demonstration, the method was used to calculate bounds on the performances of several communication systems, each based on serial concatenation of a (63,56) expurgated Hamming code with a convolutional inner code through a convolutional interleaver. The bounds calculated by use of the method were compared with results of numerical simulations of performances of the systems to show the regions where the bounds are tight (see figure).

This work was done by Bruce Moision and Samuel Dolinar of Caltech for NASA's Jet Propulsion Laboratory. Further information is contained in a TSP (see page 1). NPO-44652

Parameterizing Coefficients of a POD-Based Dynamical System

This parameterization enables accurate prediction of temporal evolution of certain flow dynamics.

Goddard Space Flight Center, Greenbelt, Maryland

A method of parameterizing the coefficients of a dynamical system based of a proper orthogonal decomposition (POD) representing the flow dynamics of a viscous fluid has been introduced. (A brief description of POD is presented in the immediately preceding article.) The present parameterization method is intended to enable construction of the dynamical system to accurately represent the temporal evolution of the flow dynamics over a range of Reynolds numbers.

The need for this or a similar method arises as follows: A procedure that includes direct numerical simulation followed by POD, followed by Galerkin projection to a dynamical system has been proven to enable representation of flow dynamics by a low-dimensional model at the Reynolds number of the simulation. However, a more difficult task is to obtain models that are valid over a range of Reynolds numbers. Extrapolation of low-dimensional models by use of straightforward Reynolds-number-based parameter continuation has proven to be inadequate for successful prediction of flows.

A key part of the problem of constructing a dynamical system to accurately represent the temporal evolution of the flow dynamics over a range of Reynolds numbers is the problem of understanding and providing for the variation of the coefficients of the dynamical system with the Reynolds number. Prior methods do not enable capture of temporal dynamics over ranges of Reynolds numbers in low-dimensional models, and are not even satisfactory when large numbers of modes are used.

The basic idea of the present method is to solve the problem through a suitable parameterization of the coefficients of the dynamical system. The parameterization computations involve utilization of the transfer of kinetic energy between modes as a function of Reynolds number. The thus-parameterized dynamical system accurately predicts the flow dynamics and is applicable to a range of flow problems in the dynamical regime around the Hopf bifurcation. Parameter-continuation software can be used on the parameterized dynamical system to derive a bifurcation diagram that accurately predicts the temporal flow behavior.

This work was done by Virginia L. Kalb of Goddard Space Flight Center. For further information, contact the Goddard Innovative Partnerships Office at (301) 286-5810. GSC-15131-1

Confidence-Based Feature Acquisition

Selective acquisition of data values enables higher classification performance at lower cost.

NASA's Jet Propulsion Laboratory, Pasadena, California

Confidence-based Feature Acquisition (CFA) is a novel, supervised learning method for acquiring missing feature values when there is missing data at both training (learning) and test (deployment) time. To train a machine learning classifier, data is encoded with a series of input features describing each item. In some applications, the training data may have missing values for some of the features, which can be acquired at a given cost. A relevant JPL example is that of the Mars rover exploration in which the features are obtained from a variety of different instruments, with different power consumption and integration time costs. The challenge is to decide which features will lead to increased classification performance and are therefore worth acquiring (paying the cost).

To solve this problem, CFA, which is made up of two algorithms (CFA-train and CFA-predict), has been designed to greedily minimize total acquisition cost (during training and testing) while aiming for a specific accuracy level (specified as a confidence threshold). With this method, it is assumed that there is a non-empty subset of features that are "free;" that is, every instance in the data set in-

cludes these features initially for zero cost. It is also assumed that the feature acquisition (FA) cost associated with each feature is known in advance, and that the FA cost for a given feature is the same for all instances. Finally, CFA requires that the base-level classifiers produce not only a classification, but also a confidence (or posterior probability).

CFA trains an ensemble of classifiers $M_0 \ldots M_f$ that use successively larger subsets of the features to classify instances. M_0 uses only the "free" (zero cost) features, and M_1 additionally incorporates costly features F_1 through F_i. CFA reduces FA cost in that model M_i is trained only on instances that cannot be classified with sufficient confidence by model M_{i-1}. Therefore, values for feature F_i are acquired only for the instances that require it. At test time, each test instance is successively classified by M_0, M_1, $M_2 \ldots$ until its classification is sufficiently confident (i.e., until the confidence of the prediction reaches the confidence threshold). Again, features are acquired for the new instance only as required. In an empirical comparison with an existing method (Cost-Sensitive Naive Bayes) that makes acquisition decisions only during test time (and therefore requires that all training items be fully acquired), CFA achieves the same (or higher) level of performance at a much reduced cost (by at least an order of magnitude).

This work was done by Kiri L. Wagstaff of Caltech and Marie desJardins and James MacGlashan of the University of Maryland for NASA's Jet Propulsion Laboratory. For more information, contact iaoffice@jpl.nasa.gov. NPO-46886

Algorithm for Lossless Compression of Calibrated Hyperspectral Imagery

NASA's Jet Propulsion Laboratory, Pasadena, California

A two-stage predictive method was developed for lossless compression of calibrated hyperspectral imagery. The first prediction stage uses a conventional linear predictor intended to exploit spatial and/or spectral dependencies in the data. The compressor tabulates counts of the past values of the difference between this initial prediction and the actual sample value. To form the ultimate predicted value, in the second stage, these counts are combined with an adaptively updated weight function intended to capture information about data regularities introduced by the calibration process. Finally, prediction residuals are losslessly encoded using adaptive arithmetic coding.

Algorithms of this type are commonly tested on a readily available collection of images from the Airborne Visible/Infrared Imaging Spectrometer (AVIRIS) hyperspectral imager. On the standard calibrated AVIRIS hyperspectral images that are most widely used for compression benchmarking, the new compressor provides more than 0.5 bits/sample improvement over the previous best compression results.

The algorithm has been implemented in Mathematica. The compression algorithm was demonstrated as beneficial on 12-bit calibrated AVIRIS images.

This work was done by Aaron B. Kiely and Matthew A. Klimesh of Caltech for NASA's Jet Propulsion Laboratory. For more information, contact iaoffice@jpl.nasa.gov. NPO-46547

Universal Decoder for PPM of any Order

Complexity can be reduced and flexibility increased, at small cost in performance.

NASA's Jet Propulsion Laboratory, Pasadena, California

A recently developed algorithm for demodulation and decoding of a pulse-position-modulation (PPM) signal is suitable as a basis for designing a single hardware decoding apparatus to be capable of handling any PPM order. Hence, this algorithm offers advantages of greater flexibility and lower cost, in comparison with prior such algorithms, which necessitate the use of a distinct hardware implementation for each PPM order. In addition, in comparison with the prior algorithms, the present algorithm entails less complexity in decoding at large orders.

An unavoidably lengthy presentation of background information, including definitions of terms, is prerequisite to a meaningful summary of this development. As an aid to understanding, the figure illustrates the relevant processes of coding, modulation, propagation, demodulation, and decoding. An M-ary PPM signal has M time slots per symbol period. A pulse (signifying 1) is transmitted during one of the time slots; no pulse (signifying 0) is transmitted during the other time slots.

The information intended to be con-

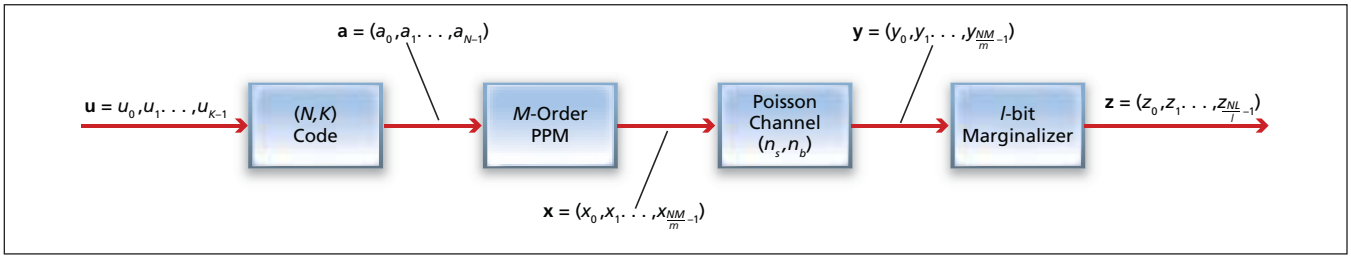

Processing of Information in an M-ary PPM communication system includes the sequence of steps depicted here. The l-bit marginalizer is a feature of the innovation reported here; the other features are typical of PPM systems in general.

veyed from the transmitting end to the receiving end of a radio or optical communication channel is a K-bit vector **u**. This vector is encoded by an (N,K) binary error-correcting code, producing an N-bit vector **a**. In turn, the vector a is subdivided into blocks of $m = \log_2(M)$ bits and each such block is mapped to an M-ary PPM symbol. The resultant coding/modulation scheme can be regarded as equivalent to a nonlinear binary code. The binary vector of PPM symbols, **x** is transmitted over a Poisson channel, such that there is obtained, at the receiver, a Poisson-distributed photon count characterized by a mean background count n_b during no-pulse time slots and a mean signal-plus-background count of n_s+n_b during a pulse time slot.

In the receiver, demodulation of the signal is effected in an iterative soft decoding process that involves consideration of relationships among photon counts and conditional likelihoods of m-bit vectors of coded bits. Inasmuch as the likelihoods of all the m-bit vectors of coded bits mapping to the same PPM symbol are correlated, the best performance is obtained when the joint m-bit conditional likelihoods are utilized. Unfortunately, the complexity of decoding, measured in the number of operations per bit, grows exponentially with m, and can thus become prohibitively expensive for large PPM orders. For a system required to handle multiple PPM orders, the cost is even higher because it is necessary to have separate decoding hardware for each order. This concludes the prerequisite background information.

In the present algorithm, the decoding process as described above is modified by, among other things, introduction of an l-bit marginalizer subalgorithm. The term "l-bit marginalizer" signifies that instead of m-bit conditional likelihoods, the decoder computes l-bit conditional likelihoods, where l is fixed. Fixing l, regardless of the value of m, makes it possible to use a single hardware implementation for any PPM order. One could minimize the decoding complexity and obtain an especially simple design by fixing l at 1, but this would entail some loss of performance. An intermediate solution is to fix l at some value, greater than 1, that may be less than or greater than m. This solution makes it possible to obtain the desired flexibility to handle any PPM order while compromising between complexity and loss of performance.

This work was done by Bruce E. Moision of Caltech for NASA's Jet Propulsion Laboratory. For more information, contact iaoffice@jpl.nasa.gov. NPO-46013

Algorithm for Stabilizing a POD-Based Dynamical System

Goddard Space Flight Center, Greenbelt, Maryland

This algorithm provides a new way to improve the accuracy and asymptotic behavior of a low-dimensional system based on the proper orthogonal decomposition (POD). Given a data set representing the evolution of a system of partial differential equations (PDEs), such as the Navier-Stokes equations for incompressible flow, one may obtain a low-dimensional model in the form of ordinary differential equations (ODEs) that should model the dynamics of the flow. Temporal sampling of the direct numerical simulation of the PDEs produces a spatial time series. The POD extracts the temporal and spatial eigenfunctions of this data set. Truncated to retain only the most energetic modes followed by Galerkin projection of these modes onto the PDEs obtains a dynamical system of ordinary differential equations for the time-dependent behavior of the flow.

In practice, the steps leading to this system of ODEs entail numerically computing first-order derivatives of the mean data field and the eigenfunctions, and the computation of many inner products. This is far from a perfect process, and often results in the lack of long-term stability of the system and incorrect asymptotic behavior of the model. This algorithm describes a new stabilization method that utilizes the temporal eigenfunctions to derive correction terms for the coefficients of the dynamical system to significantly reduce these errors.

This work was done by Virginia L. Kalb of Goddard Space Flight Center. For further information, contact the Goddard Innovative Partnerships Office at (301) 286-5810. GSC-15129-1

Mission Reliability Estimation for Repairable Robot Teams

An analytical model demonstrates autonomous and intelligent control systems capable of operating distributed, multi-planetary surface vehicles for scouting or construction.

NASA's Jet Propulsion Laboratory, Pasadena, California

A mission reliability estimation method has been designed to translate mission requirements into choices of robot modules in order to configure a multi-robot team to have high reliability at minimal cost. In order to build cost-effective robot teams for long-term missions, one must be able to compare alternative design paradigms in a principled way by comparing the reliability of different robot models and robot team configurations. Core modules have been created including: a probabilistic module with reliability-cost characteristics, a method for combining the characteristics of multiple modules to determine an overall reliability-cost characteristic, and a method for the generation of legitimate module combinations based on mission specifications and the selection of the best of the resulting combinations from a cost-reliability standpoint.

The developed methodology can be used to predict the probability of a mission being completed, given information about the components used to build the robots, as well as information about the mission tasks. In the research for this innovation, sample robot missions were examined and compared to the performance of robot teams with different numbers of robots and different numbers of spare components.

Data that a mission designer would need was factored in, such as whether it would be better to have a spare robot versus an equivalent number of spare parts, or if mission cost can be reduced while maintaining reliability using spares.

This analytical model was applied to an example robot mission, examining the cost-reliability tradeoffs among different team configurations. Particularly scrutinized were teams using either redundancy (spare robots) or repairability (spare components). Using conservative estimates of the cost-reliability relationship, results show that it is possible to significantly reduce the cost of a robotic mission by using cheaper, lower-reliability components and providing spares. This suggests that the current design paradigm of building a minimal number of highly robust robots may not be the best way to design robots for extended missions.

This work was done by Ashitey Trebi-Ollennu of Caltech and John Dolan and Stephen Stancliff of Carnegie Mellon University for NASA's Jet Propulsion Laboratory. Further information is contained in a TSP (see page 1).

The software used in this innovation is available for commercial licensing. Please contact Karina Edmonds of the California Institute of Technology at (626) 395-2322. Refer to NPO-44825.

Software

Processing AIRS Scientific Data Through Level 3

The Atmospheric Infra-Red Sounder (AIRS) Science Processing System (SPS) is a collection of computer programs, known as product generation executives (PGEs). The AIRS SPS PGEs are used for processing measurements received from the AIRS suite of infrared and microwave instruments orbiting the Earth onboard NASA's Aqua spacecraft. Early stages of the AIRS SPS development were described in a prior *NASA Tech Briefs* article: "Initial Processing of Infrared Spectral Data" (NPO-35243), Vol. 28, No. 11 (November 2004), page 39.

In summary: Starting from Level 0 (representing raw AIRS data), the AIRS SPS PGEs and the data products they produce are identified by alphanumeric labels (1A, 1B, 2, and 3) representing successive stages or levels of processing. The previous *NASA Tech Briefs* article described processing through Level 2, the output of which comprises geo-located atmospheric data products such as temperature and humidity profiles among others. The AIRS Level 3 PGE samples selected information from the Level 2 standard products to produce a single global gridded product. One Level 3 product is generated for each day's collection of Level 2 data. In addition, daily Level 3 products are aggregated into two multi-day products: an eight-day (half the orbital repeat cycle) product and monthly (calendar month) product.

This work was done by Stephanie Granger, Robert Oliphant, and Evan Manning of Caltech for NASA's Jet Propulsion Laboratory. Further information is contained in a TSP (see page 1).

This software is available for commercial licensing. Please contact Karina Edmonds of the California Institute of Technology at (626) 395-2322. Refer to NPO-42146.

Web-Based Requesting and Scheduling Use of Facilities

Automated User's Training Operations Facility Utilization Request (AutoFUR) is prototype software that administers a Web-based system for requesting and allocating facilities and equipment for astronaut-training classes in conjunction with scheduling the classes. AutoFUR also has potential for similar use in such applications as scheduling flight-simulation equipment and instructors in commercial airplane-pilot training, managing preventive-maintenance facilities, and scheduling operating rooms, doctors, nurses, and medical equipment for surgery.

Whereas requesting and allocation of facilities was previously a manual process that entailed examination of documents (including paper drawings) from different sources, AutoFUR partly automates the process and makes all of the relevant information available via the requester's computer. By use of AutoFUR, an instructor can fill out a facility-utilization request (FUR) form on line, consult the applicable flight manifest(s) to determine what equipment is needed and where it should be placed in the training facility, reserve the corresponding hardware listed in a training-hardware inventory database, search for alternative hardware if necessary, submit the FUR for processing, and cause paper forms to be printed. AutoFUR also maintains a searchable archive of prior FURs.

This program was written by Carolyn M. Yeager of Aptek, Inc., for Johnson Space Center. Further information is contained in a TSP (see page 1). MSC-23247-1

AutoGen Version 5.0

Version 5.0 of the AutoGen software has been released. Previous versions, variously denoted "Autogen" and "autogen," were reported in two articles: "Automated Sequence Generation Process and Software" (NPO-30746), *Software Tech Briefs* (Special Supplement to *NASA Tech Briefs*), September 2007, page 30, and "Autogen Version 2.0" (NPO-41501), *NASA Tech Briefs*, Vol. 31, No. 10 (October 2007), page 58.

To recapitulate: AutoGen (now signifying "automatic sequence generation") automates the generation of sequences of commands in a standard format for uplink to spacecraft. AutoGen requires fewer workers than are needed for older manual sequence-generation processes, and greatly reduces sequence-generation times.

The sequences are embodied in spacecraft activity sequence files (SASFs). AutoGen automates generation of SASFs by use of another previously reported program called "APGEN." AutoGen encodes knowledge of different mission phases and of how the resultant commands must differ among the phases. AutoGen also provides means for customizing sequences through use of configuration files. The approach followed in developing AutoGen has involved encoding the behaviors of a system into a model and encoding algorithms for context-sensitive customizations of the modeled behaviors.

This version of AutoGen addressed the MRO (Mars Reconnaissance Orbiter) primary science phase (PSP) mission phase. On previous Mars missions this phase has more commonly been referred to as mapping phase. This version addressed the unique aspects of sequencing orbital operations and specifically the mission specific adaptation of orbital operations for MRO. This version also includes capabilities for MRO's role in Mars relay support for UHF relay communications with the MER rovers and the Phoenix lander.

This program was written by Roy E. Gladden, Teerapat Khanampornpan, and Forest W. Fisher of Caltech for NASA's Jet Propulsion Laboratory.

This software is available for commercial licensing. Please contact Karina Edmonds of the California Institute of Technology at (626) 395-2322. Refer to NPO-45984

Time-Tag Generation Script

Time-Tag Generation Script (TTaGS) is an application program, written in the AWK scripting language, for generating commands for aiming one Ku-band antenna and two S-band antennas for communicating with spacecraft. TTaGS saves between 2 and 4 person-hours per every 24 hours by automating the repetitious process of building between 150 and 180 antenna-control commands. TTaGS reads a text database of communication-satellite schedules and a text database of satellite rise and set times and cross-references items in the two databases. It then compares the scheduled start and stop with the geometric rise and set to compute the times to execute antenna control commands. While so doing, TTaGS determines whether to generate commands for guidance, navigation,

and control computers to tell them which satellites to track.

To help prevent Ku-band irradiation of the Earth, TTaGS accepts input from the user about horizon tolerance and accordingly restricts activation and effects deactivation of the transmitter. TTaGS can be modified easily to enable tracking of additional satellites and for such other tasks as reading Sun-rise/set tables to generate commands to point the solar photovoltaic arrays of the International Space Station at the Sun.

This program was written by Dan E. Jackson of Barrios Technology for Johnson Space Center. For further information, contact the Johnson Commercial Technology Office at (281) 483-3809. MSC-23588-1

PPM Receiver Implemented in Software

A computer program has been written as a tool for developing optical pulse-position-modulation (PPM) receivers in which photodetector outputs are fed to analog-to-digital converters (ADCs) and all subsequent signal processing is performed digitally. The program can be used, for example, to simulate an all-digital version of the PPM receiver described in "Parallel Processing of Broad-Band PPM Signals" (NPO-40711), which appears elsewhere in this issue of *NASA Tech Briefs*. The program can also be translated into a design for digital PPM-receiver hardware.

The most notable innovation embodied in the software and the underlying PPM-reception concept is a digital processing subsystem that performs synchronization of PPM time slots, even though the digital processing is, itself, asynchronous in the sense that no attempt is made to synchronize it with the incoming optical signal *a priori* and there is no feedback to analog signal-processing subsystems or ADCs. Functions performed by the software receiver include time-slot synchronization, symbol synchronization, coding preprocessing, and diagnostic functions. The program is written in the MATLAB® and Simulink® software system. The software receiver is highly parameterized and, hence, programmable: for example, slot- and symbol-synchronization filters have programmable bandwidths.

This program was written by Andrew Gray, Edward Kang, Norman Lay, Victor Vilnrotter, Meera Srinivasan, and Clement Lee of Caltech for NASA's Jet Propulsion Laboratory.

In accordance with Public Law 96-517, the contractor has elected to retain title to this invention. Inquiries concerning rights for its commercial use should be addressed to:

Innovative Technology Assets Management
JPL
Mail Stop 202-233
4800 Oak Grove Drive
Pasadena, CA 91109-8099
E-mail: iaoffice@jpl.nasa.gov

Refer to NPO-40712, volume and number of this NASA Tech Briefs *issue, and the page number.*

Tropospheric Emission Spectrometer Product File Readers

TES Product File Reader software extracts data from publicly available Tropospheric Emission Spectrometer (TES) HDF (Hierarchical Data Format) product data files using publicly available format specifications for scientific analysis in IDL (interactive data language). In this innovation, the software returns data fields as simple arrays for a given file. A file name is provided, and the contents are returned as simple IDL variables.

This work was done by Brendan M. Fisher of Caltech for NASA's Jet Propulsion Laboratory. For more information, see http://tes.jpl.nasa.gov/.

This software is available for commercial licensing. Please contact Karina Edmonds of the California Institute of Technology at (626) 395-2322. Refer to NPO-47000.

Reporting Differences Between Spacecraft Sequence Files

A suite of computer programs, called "seq diff suite," reports differences between the products of other computer programs involved in the generation of sequences of commands for spacecraft. These products consist of files of several types: replacement sequence of events (RSOE), DSN keyword file [DKF (wherein "DSN" signifies "Deep Space Network)], spacecraft activities sequence file (SASF), spacecraft sequence file (SSF), and station allocation file (SAF). These products can include line numbers, request identifications, and other pieces of information that are not relevant when generating command sequence products, though these fields can result in the appearance of many changes to the files, particularly when using the UNIX diff command to inspect file differences. The outputs of prior software tools for reporting differences between such products include differences in these non-relevant pieces of information.

In contrast, seq diff suite removes the fields containing the irrelevant pieces of information before processing to extract differences, so that only relevant differences are reported. Thus, seq diff suite is especially useful for reporting changes between successive versions of the various products and in particular flagging difference in fields relevant to the sequence command generation and review process.

This program was written by Teerapat Khanampornpan, Roy E. Gladden, and Forest W. Fisher of Caltech for NASA's Jet Propulsion Laboratory.

This software is available for commercial licensing. Please contact Karina Edmonds of the California Institute of Technology at (626) 395-2322. Refer to NPO-45438.

Coordinating "Execute" Data for ISS and Space Shuttle

The Joint Execute Package Development and Integration tool is a Web utility program that provides an integrated capability to generate and manage messages and "execute" package data for members of a space shuttle and the International Space Station (ISS). (An "execute" package consists of flight plans, short-term plans, procedure updates, data needed to operate the space-shuttle and ISS systems, in-flight maintenance procedures, inventory-stowage data, software upgrades, flight notes, scripts for publicized events, and other instructions.) This program is a third-generation "execute"-package Web tool, built on experience gained from two programs used previously to support realtime operations.

This program provides integration and synchronization between the space-shuttle and ISS teams during joint operations. Hundreds of messages per week must be uplinked as "joint" messages; that is, messages for crewmembers of both spacecraft. The program includes configuration-management components that ensure that the same message goes to both crews and spacecraft, effectively eliminating the potential for error in manual direction of messages. The program also controls the format and layout of the crews' Web pages, ensuring consistency between uplinks. If the crews' Web pages were edited man-

ually, hyperlink and formatting errors would be common.

This program was written by Greg Whitney of Johnson Space Center, David Melendrez of Barrios Technology, and Jason Hadlock of United Space Alliance. MSC-23601-1

Database for Safety-Oriented Tracking of Chemicals

SafetyChem is a computer program that maintains a relational database for tracking chemicals and associated hazards at Johnson Space Center (JSC) by use of a Web-based graphical user interface. The SafetyChem database is accessible to authorized users via a JSC intranet. All new chemicals pass through a safety office, where information on hazards, required personal protective equipment (PPE), fire-protection warnings, and target organ effects (TOEs) is extracted from material safety data sheets (MSDSs) and recorded in the database.

The database facilitates real-time management of inventory with attention to such issues as stability, shelf life, reduction of waste through transfer of unused chemicals to laboratories that need them, quantification of chemical wastes, and identification of chemicals for which disposal is required. Upon searching the database for a chemical, the user receives information on physical properties of the chemical, hazard warnings, required PPE, a link to the MSDS, and references to the applicable International Standards Organization (ISO) 9000 standard work instructions and the applicable job hazard analysis. Also, to reduce the labor hours needed to comply with reporting requirements of the Occupational Safety and Health Administration, the data can be directly exported into the JSC hazardous-materials database.

This program was written by Jacob Stump, Sandra Carr, Debrah Plumlee, Andy Slater, Thomas M. Samson, and Toby L. Holowaty of Wyle Laboratories and Darren Skeete, Mary Alice Haenz, Scot Hershman, and Pushpa Raviprakash of Science Applications International Corp. for Johnson Space Center. For further information, contact the Johnson Commercial Technology Office at (281) 483-3809. MSC-23627-1

Apparatus for Cold, Pressurized Biogeochemical Experiments

Bacteria are grown under conditions imitating those at ocean depths.

NASA's Jet Propulsion Laboratory, Pasadena, California

A laboratory apparatus has been devised as a means of studying plausible biogeochemical reactions under high-pressure, low-temperature aqueous, anaerobic conditions like those conjectured to prevail in a liquid water ocean on Europa (the fourth largest moon of the planet Jupiter). The experiments to be performed by use of this apparatus are intended to enhance understanding of how life (if any) could originate and evolve in the Europa ocean environment. Inasmuch as terrestrial barophilic, psychrophilic organisms that thrive under anaerobic conditions are used in the experiments, the experiments may also contribute to terrestrial biogeochemistry.

The apparatus (see figure) includes a bolt-closure reaction vessel secured inside a refrigerator that maintains a temperature of 4 °C. Pressurized water is supplied to the interior of the vessel by a hydrostatic pump, which is attached to the vessel via high-pressure fittings.

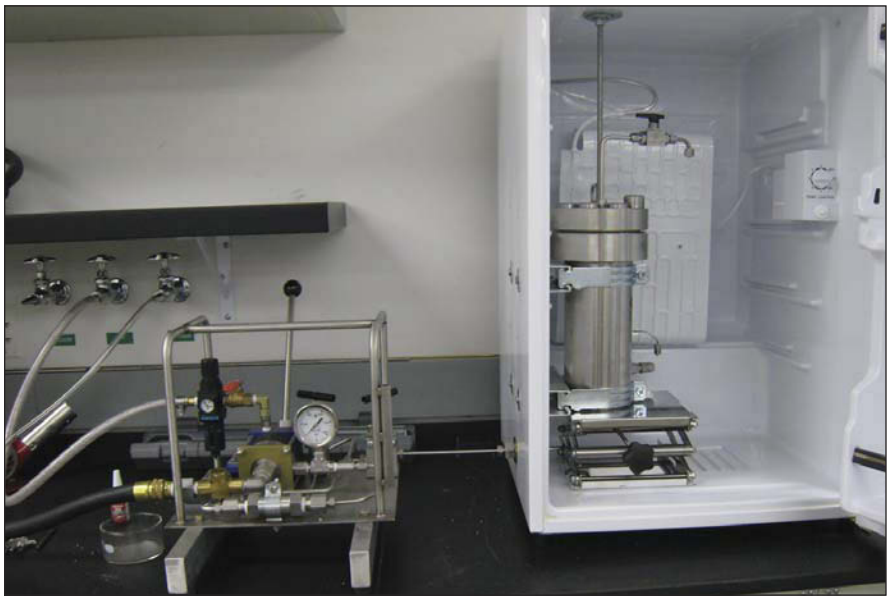

This **Laboratory Apparatus** is used to study biogeochemical reactions in liquid water at high pressure and low temperature. Bacterial specimens are loaded from the top of the vessel into sample cells equipped with 0.2-μm filters. The vessel is filled with water, air is vented from the top through a valve, and then the water is pressurized to 5 kpsi (≈34 MPa).

The terrestrial organisms used in the experiments thus far have been several facultative barophilic, psychrophilic stains of *Shewanella* bacteria. In the experiments, these organisms have been tested for reduction of ferric ion by growing them in the presence of a ferric food source under optimized terrestrial conditions. The short-term goal of these experiments has been to select *Shewanella* strains that exhibit iron-reduction capability and test their ability to facilitate biogeochemical reduction of iron under temperature and pressure conditions imitating those in Europa's ocean. It is anticipated, that, once growth under Europa-like conditions has been achieved, the selected *Shewanella* strains will be used to facilitate biogeochemical reactions of sulfate and carbonate with hydrogen gas. Any disequilibrium of the products with the environment would be interpreted as signifying biogenic activity and the possibility of life in Europa's ocean.

This work was done by Xenia Amashukeli, Robert T. Pappalardo, and Stephanie A. Connon of Caltech and Damhnait F. Gleeson of the University of Colorado for NASA's Jet Propulsion Laboratory. For more information contact iaoffice@jpl.nasa.gov
NPO-45538

Growing B Lymphocytes in a Three-Dimensional Culture System

Cells grown in this system live long and closely resemble in vivo cells.

Lyndon B. Johnson Space Center, Houston, Texas

A three-dimensional (3D) culture system for growing long-lived B lymphocytes has been invented. The capabilities afforded by the system can be expected to expand the range of options for immunological research and related activities, including testing of immunogenicity of vaccine candidates *in vitro*, generation of human monoclonal antibodies, and immunotherapy.

Mature lymphocytes, which are the effectors of adaptive immune responses in vertebrates, are extremely susceptible to apoptotic death, and depend on continuous reception of survival-inducing stimulation (in the forms of cytokines, cell-to-cell contacts, and antigen receptor signaling) from the microenvironment. For this reason, efforts to develop systems for long-term culture of functional, non-transformed and non-activated mature lymphocytes have been unsuccessful until now.

The bone-marrow microenvironment supports the growth and differentiation of many hematopoietic lineages, in addition to B-lymphocytes. Primary bone-marrow cell cultures designed to promote the development of specific cell types *in vitro* are highly desirable experimental systems, amenable to manipulation under controlled conditions. However, the dynamic and complex network of stromal cells and insoluble matrix proteins is disrupted in prior plate- and flask-based culture systems, wherein the microenvironments have a predominantly two-dimensional (2D) character. In 2D bone-marrow cultures, normal B-lymphoid cells become progressively skewed toward precursor B-cell populations that do not retain a normal immunophenotype, and such mature B-lymphocytes as those harvested from the spleen or lymph nodes do not survive beyond several days *ex vivo* in the absence of mitogenic stimulation.

The present 3D culture system is a bioreactor that contains highly porous artificial scaffolding that supports the long-term culture of bone marrow, spleen, and lymph-node samples. In this system, unlike in 2D culture systems, B-cell subpopulations developing within 3D cultures that have been modified to foster lymphopoiesis retain an immunophenotype that closely recapitulates cells in fresh bone marrow harvests. The 3D culture system has been found to be capable of supporting long-lived (8 weeks) populations of B and T lymphocytes from peripheral lymphoid organs, in the absence of activation signals, to an extent not achievable by conventional culture techniques. Interestingly, it has been found that 3D-culture B cells display a phenotype that has characteristics of both B1a and B2 cells. These promising preliminary observations suggest that the 3D culture system could be used with success in the study of peripheral-B-lymphocyte biology and in the development of biotechnological techniques and processes.

This work was done by J. H. David Wu and Andrea Bottaro of the University of Rochester for Johnson Space Center. For further information, contact the Johnson Commercial Technology Office at (281) 483-3809.

In accordance with Public Law 96-517, the contractor has elected to retain title to this invention. Inquiries concerning rights for its commercial use should be addressed to:

University of Rochester, Chemical Engineering
518 Hylan Building
P.O. Box 270140
Rochester, NY 14627-0140
Phone No.: (585) 275-3998
Web: www.rochester.edu/ott/

Refer to MSC-23571-1, volume and number of this Medical Design Briefs *issue, and the page number.*

Tissuelike 3D Assemblies of Human Broncho-Epithelial Cells

Experimental conditions are more realistic than those of 2D monolayer cell cultures.

Lyndon B. Johnson Space Center, Houston, Texas

Three-dimensional (3D) tissuelike assemblies (TLAs) of human broncho-epithelial (HBE) cells have been developed for use in *in vitro* research on infection of humans by respiratory viruses. The 2D monolayer HBE cell cultures heretofore used in such research lack the complex cell structures and interactions characteristic of *in vivo* tissues and, consequently, do not adequately emulate the infection dynamics of *in-vivo* microbial adhesion and invasion. In contrast, the 3D HBE TLAs are characterized by more-realistic reproductions of the geometrical and functional complexity, differentiation of cells, cell-to-cell interactions, and cell-to-matrix interactions characteristic of human respiratory epithelia. Hence, the 3D HBE TLAs are expected to make it possible to perform at least some of the research *in vitro* under more-realistic conditions, without need to infect human subjects.

The TLAs are grown on collagen-coated cyclodextran microbeads under controlled conditions in a nutrient liquid in the simulated microgravitational environment of a bioreactor of the rotating-wall-vessel type. Primary human mesenchymal bronchial-tracheal cells are used as a foundation matrix, while adult human bronchial epithelial immortalized cells are used as the overlying component. The beads become coated with cells, and cells on adjacent beads coalesce into 3D masses. The resulting TLAs have been found to share significant characteristics with *in vivo* human respiratory epithelia including polarization, tight junctions, desmosomes, and microvilli. The differentiation of the cells in these TLAs into tissues functionally similar to *in vivo* tissues is confirmed by the presence of

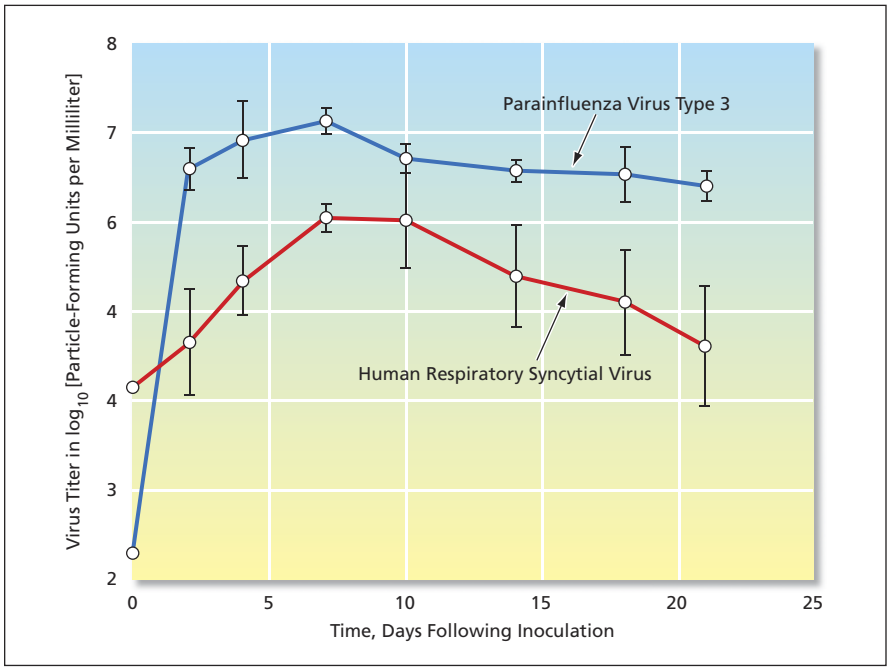

These **Virus Titers** indicate rapid growth of virus populations during the first few days.

tissuelike differentiation marker compounds, including villin, keratins, and specific lung epithelium marker compounds, and by the production of tissue mucin.

In a series of initial infection tests, TLA cultures were inoculated with human respiratory syncytial viruses and parainfluenza type 3 viruses. Infection was confirmed by photomicrographs that showed signs of damage by viruses and virus titers (see figure) that indicated large increases in the populations of viruses during the days following inoculation.

This work was done by Thomas J. Goodwin of Johnson Space Center. Further information is contained in a TSP (see page 1).

This invention is owned by NASA, and a patent application has been filed. Inquiries concerning nonexclusive or exclusive license for its commercial development should be addressed to the Patent Counsel, Johnson Space Center, (281) 483-0837. Refer to MSC-24164-1.

Isolation of Resistance-Bearing Microorganisms

NASA's Jet Propulsion Laboratory, Pasadena, California

Strategies were explored for inactivating resistance-bearing microorganisms, focusing on a new species (*Bacillus horneckii* sp. nov.) discovered on the surfaces of the Kennedy Space Center cleanroom facility in which the Phoenix lander was assembled. Two strains that belong to this novel species were isolated and subjected to a comprehensive, polyphasic analysis to characterize their taxonomic position.

Both phenotypic and genotypic analyses clearly indicate that these isolates belong to the genus *Bacillus*, and represent a novel species. In addition to the phylogenetic affiliation, structurally the spores of this novel bacterium possess an extraneous layer, which might be responsible for increased resistance to space radiation conditions. The chemical characterization of this novel, extraneous layer of spores will reveal the mechanisms behind radiation resistance.

This work was done by Kasthuri J. Venkateswaran, Alexander Probst, Parag A. Vaishampayan, and Sudeshna Ghosh of Caltech; and Shariff Osman of Lawrence Berkeley National Laboratory for NASA's Jet Propulsion Laboratory. For more information, contact iaoffice@jpl.nasa.gov. NPO-46337

Oscillating Cell Culture Bioreactor

This bioreactor is well suited to work with different biological specimens.

Lyndon B. Johnson Space Center, Houston, Texas

To better exploit the principles of gas transport and mass transport during the processes of cell seeding of 3D scaffolds and *in vitro* culture of 3D tissue engineered constructs, the oscillatory cell culture bioreactor provides a flow of cell suspensions and culture media directly through a porous 3D scaffold (during cell seeding) and a 3D construct (during subsequent cultivation) within a highly gas-permeable closed-loop tube. This design is simple, modular, and flexible, and its component parts are easy to assemble and operate, and are inexpensive. Chamber volume can be very low, but can be easily scaled up. This innovation is well suited to work with different biological specimens, particularly with cells having high oxygen requirements and/or shear sensitivity, and different scaffold structures and dimensions.

The closed-loop changer is highly gas permeable to allow efficient gas exchange during the cell seeding/culturing process. A porous scaffold, which may be seeded with cells, is fixed by means of a scaffold holder to the chamber wall with scaffold/construct orientation with respect to the chamber determined by the geometry of the scaffold holder. A fluid, with/without biological specimens, is added to the chamber such that all, or most, of the air is displaced (i.e., with or without an enclosed air bubble). Motion is applied to the chamber within a controlled environment (e.g., oscillatory motion within a humidified 37 °C incubator). Movement of the chamber induces relative motion of the scaffold/construct with respect to the fluid. In case the fluid is a cell suspension, cells will come into contact with the scaffold and eventually adhere to it. Alternatively, cells can be seeded on scaffolds by gel entrapment prior to bioreactor cultivation.

Subsequently, the oscillatory cell culture bioreactor will provide efficient gas exchange (i.e., of oxygen and carbon dioxide, as required for viability of metabolically active cells) and controlled levels of fluid dynamic shear (i.e., as required for viability of shear-sensitive cells) to the developing engineered tissue construct.

This bioreactor was recently utilized to show independent and interactive effects of a growth factor (IGF-I) and slow bidirectional perfusion on the survival, differentiation, and contractile performance of 3D tissue engineering cardiac constructs.

The main application of this system is within the tissue engineering industry. The ideal final application is within the automated mass production of tissue-engineered constructs. Target industries could be both life sciences companies as well as bioreactor device producing companies.

This work was done by Lisa E. Freed, Mingyu Cheng, and Matteo G. Moretti of Massachusetts Institute of Technology for Johnson Space Center. For further information, contact the Johnson Technology Transfer Office at (281) 483-3809.

In accordance with Public Law 96-517, the contractor has elected to retain title to this invention. Inquiries concerning rights for its commercial use should be addressed to:

Patent Compliance Administrator
Massachusetts Institute of Technology
Five Cambridge Center, Kendall Square
Room NE25-230
Cambridge, MA 021142-1493

Refer to MSC-24270-1, volume and number of this Medical Design Briefs *issue, and the page number.*

Liquid Cooling/Warming Garment

This lightweight garment can be used by firefighters, soldiers, and personnel working with hazardous materials.

The NASA liquid cooling/ventilating garment (LCVG) currently in use was developed over 40 years ago. With the commencement of a greater number of extra-vehicular activity (EVA) procedures with the construction of the International Space Station, problems of astronaut comfort, as well as the reduction of the consumption of energy, became more salient.

A shortened liquid cooling/warming garment (SLCWG) has been developed based on physiological principles comparing the efficacy of heat transfer of different body zones; the capability of blood to deliver heat; individual muscle and fat body composition as a basis for individual thermal profiles to customize the zonal sections of the garment; and the development of shunts to minimize or redirect the cooling/warming loop for different environmental conditions, physical activity levels, and emergency situations.

The SLCWG has been designed and completed, based on extensive testing in rest, exercise, and antiorthostatic conditions. It is more energy efficient than the LCVG currently used by NASA. The total length of tubing in the SLCWG is approximately 35 percent less and the weight decreased by 20 percent compared to the LCVG.

The novel features of the innovation are:

1. The efficiency of the SLCWG to maintain thermal status under extreme changes in body surface temperatures while using significantly less tubing than the LCVG.
2. The construction of the garment based on physiological principles of heat transfer.
3. The identification of the body areas that are most efficient in heat transfer.
4. The inclusion of a hood as part of the garment.
5. The lesser consumption of energy.

This work was done by Victor S. Koscheyev, Gloria R. Leon, and Michael J. Dancisak of the University of Minnesota for Johnson Space Center. For further information, contact the JSC Innovation Partnerships Office at (281) 483-3809.

In accordance with Public Law 96-517, the contractor has elected to retain title to this invention. Inquiries concerning rights for its commercial use should be addressed to:

Victor S. Koscheyev, M.D., Ph.D.
Department of Kinesiology
University of Minnesota, Cooke Hall
1900 University Ave., S.E.
Minneapolis, MN 55455

Refer to MSC-24352-1, volume and number of this Medical Design Briefs *issue, and the page number.*

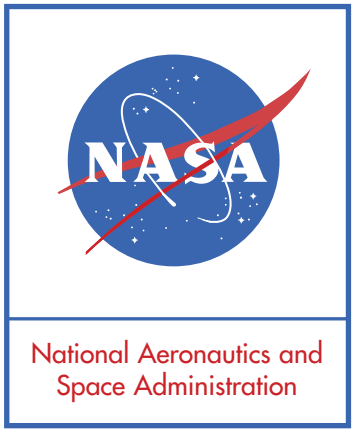
NASA
National Aeronautics and
Space Administration